

## THE GIANT CARDIAC MEMBRANE PATCH METHOD: STIMULATION OF OUTWARD $\text{Na}^+$ – $\text{Ca}^{2+}$ EXCHANGE CURRENT BY MgATP

By ANTHONY COLLINS, AVRIL V. SOMLYO\*  
AND DONALD W. HILGEMANN

*From the Department of Physiology, University of Texas Southwestern Medical Center, 5323 Harry Hines Blvd, Dallas, TX 75235-9040 and \*Department of Physiology, University of Virginia, School of Medicine, 1300 Jefferson Park Avenue, Charlottesville, Virginia 22908, USA*

(Received 3 September 1990)

### SUMMARY

1. A giant patch method was used to study the stimulatory effect of cytoplasmic MgATP on outward  $\text{Na}^+$ – $\text{Ca}^{2+}$  exchange current in inside-out cardiac membrane patches (1–10 G $\Omega$  seals with 14–24  $\mu\text{m}$  pipette tip diameters) excised from guinea-pig, rabbit and mouse myocytes.

2. To establish the validity of the method with respect to structure, bleb formation was examined with electron microscopy and with confocal fluorescence light microscopy. The blebs, which form as the sarcolemma detaches, excluded intracellular organelles and transverse tubules. The blebbed cells contained normal sarcomeres, sarcoplasmic reticulum, triads and diads.

3. To further establish the validity of the method for ion transport studies, measurements of  $\text{Na}^+$ – $\text{K}^+$  pump currents and charge movements are described briefly which demonstrate (i) free access to the cytoplasmic membrane side, (ii) MgATP dependence comparable to reconstituted pump ( $K_d$ , 94  $\mu\text{M}$ ), (iii) fast, rigorous concentration control and (iv)  $\text{Na}^+$ – $\text{K}^+$  pump densities in the range of whole-cell densities.

4. Stimulation of outward  $\text{Na}^+$ – $\text{Ca}^{2+}$  exchange current by MgATP attenuated exchange current decay during step increments of cytoplasmic sodium, shifted the secondary activation of outward exchange current by cytoplasmic calcium to lower free calcium concentrations and, particularly in mouse cardiac sarcolemma, induced cytoplasmic calcium-independent current.

5. Upon removal of MgATP the stimulatory effect usually decayed with a  $t_{50}$  (half-time) of about 3 min. However, the reversal took place much more rapidly ( $t_{50}$ , 5–20 s) in patches from individual guinea-pig and rabbit myocyte batches. When decay was rapid, secondary activation by cytoplasmic calcium was shifted to higher free cytoplasmic calcium concentrations ( $K_d$ , 10–65  $\mu\text{M}$ -free calcium).

6. With repeated applications of MgATP the rate and magnitude of the stimulatory effect progressively decreased.

7. The  $K_d$  for MgATP of the initial rate of stimulation of outward exchange current was 3 mM or greater. When decay was rapid, the steady-state dependence of exchange current on MgATP also had a  $K_d$  of 3 mM or greater.

8. Stimulation of  $\text{Na}^+$ - $\text{Ca}^{2+}$  exchange current by MgATP occurred in the absence of cytoplasmic calcium with 9 mM-EGTA.

9. The stimulatory effect of 2 mM-MgATP was not inhibited by up to 200  $\mu\text{M}$  of the protein kinase inhibitor 1-(5-isoquinoline sulphonyl)-2-methylpiperazine (H7), or by peptide inhibitors of cyclic AMP-dependent protein kinase, protein kinase C and calcium-calmodulin-dependent protein kinase II.

10. The stimulatory effect of MgATP was not mimicked by MgATP- $\gamma$ -S, and it was not reversed by acid phosphatase, alkaline phosphatase or an isolated cardiac protein phosphatase. Further, the effect was not enhanced nor was decay of the effect prolonged by 2  $\mu\text{M}$  of the phosphatase inhibitor, okadaic acid.

11. We conclude that stimulation of  $\text{Na}^+$ - $\text{Ca}^{2+}$  exchange current in excised sarcolemmal patches by MgATP is not a calcium-dependent process and probably does not involve protein kinases.

#### INTRODUCTION

The  $\text{Na}^+$ - $\text{Ca}^{2+}$  exchange process in heart has been extensively studied in sarcolemmal vesicles (for review, see Reeves & Philipson, 1989), as well as in intact tissue (Hilgemann, 1986) and in isolated cardiac myocytes using whole-cell voltage clamp (Kimura, Noma & Irisawa, 1986; Kimura, Miyamae & Noma, 1987; Fedida, Noble & Shimoni, 1987; Campbell, Giles & Robinson, 1988; Egan, Noble & Noble, 1989; Earm, Ho & So, 1989) and optical methods (Barceñas-Ruiz, Beuckelmann & Wier, 1987; Crespo, Grantham & Cannell, 1990). Many properties of the exchanger are consistent among these different experimental approaches; for example, rates of sodium-dependent calcium efflux during repolarization and the accompanying action potential changes were well explained by the current densities of the inward exchange current found in myocytes (Hilgemann & Noble, 1987). However, despite these extensive studies many inconsistencies and unanswered questions remain about  $\text{Na}^+$ - $\text{Ca}^{2+}$  exchange function. For example, this exchanger in intact cells appears to be regulated secondarily by internal calcium (Kimura *et al.* 1987) and ATP (Haworth, Goknur, Hunter, Hegge & Berkoff, 1987), similarly to the squid axon exchanger but in contrast to conclusions from cardiac vesicle studies. Although the development of pipette perfusion techniques improved greatly the utility of whole-cell patch-clamp techniques for transport studies (Soejima & Noma, 1984), it appeared advantageous to develop a method with free access to the cytoplasmic side, while maintaining the exchange system in a more physiological state than appears to be the case with sarcolemmal vesicles. The first part of this article presents details of the recently developed experimental methods (Hilgemann, 1989, 1990) which enable the study of  $\text{Na}^+$ - $\text{Ca}^{2+}$  exchange current in excised patches of cardiac sarcolemma.

Remarkably little is known about physiological modulation of  $\text{Na}^+$ - $\text{Ca}^{2+}$  exchange, except as a result of changes of cytoplasmic calcium and sodium concentrations. One possible connection to regulatory systems is given by the stimulatory effect of MgATP on  $\text{Na}^+$ - $\text{Ca}^{2+}$  exchange which has been reported in squid giant axon (Baker & McNaughton, 1976; for review see DiPolo & Beaugé, 1988), barnacle muscle (Nelson & Blaustein, 1981), ferret erythrocytes (Frame & Milanick, 1990), cardiac

myocytes (Haworth *et al.* 1987), and giant excised cardiac sarcolemmal patches (Hilgemann, 1990). This type of modulation has also been reported in cardiac sarcolemmal vesicles (Caroni & Carafoli, 1983), although other laboratories have not obtained comparable results (Reeves & Philipson, 1989). While it is not expected that  $\text{Na}^+ - \text{Ca}^{2+}$  exchange activity would be regulated physiologically by changes in intracellular ATP concentration, it is conceivable that the ATP-dependent process itself may be subject to regulation via one or more physiological mechanisms such as a protein kinase system, for example. Indeed, while the mechanism of this effect is not well established, evidence for the involvement of a phosphorylation has been presented (Caroni & Carafoli, 1983; DiPolo & Beaugé, 1987*a, b*). As described in the present report, a number of attempts to implicate the involvement of a protein kinase in the excised patch system have been unsuccessful, and so it seems likely that ATP is acting via some alternative mechanism. Evidence for one such mechanism is presented in an accompanying article (Hilgemann & Collins, 1992).

#### METHODS

##### *Myocyte preparation*

The giant patch technique was employed as described in previous reports (Hilgemann, 1989, 1990). The following description includes further details, a few advantageous modifications and notable observations of a methodological nature.

Guinea-pigs and mice were heavily anaesthetized by intraperitoneal injection of pentobarbitone; rabbits were killed by decapitation for the purposes of other experimentation. Hearts were then rapidly removed and transferred to a Langendorff-type perfusion apparatus. Myocytes were isolated by standard retrograde, nominally calcium-free perfusion of isolated hearts for 20 min at 37 °C with collagenase (0.2 mg/ml Yakult (Japan) YK-101, or 1 mg/ml Worthington (USA) type 2, or a combination of both). Digestion procedures which allowed gigaohm seal formation with conventional methods also allowed formation of giant patches. Using the cell treatment procedure described subsequently, the highest yields of cells with large-scale membrane separations from myofilaments and extensive sarcolemmal blebbing were obtained in the cell batches with the highest yields of relaxed myocytes.

Digested tissue segments were placed in a 'storage solution' of the following composition: 150 mM-KCl, 10 mM-EGTA, 2 mM- $\text{MgCl}_2$ , 20 mM-dextrose, 15 mM-HEPES, and set to pH 7.2 with KOH (chemical abbreviations used in this manuscript: ethyleneglycol-bis( $\beta$ -aminoethyl-ether)*N,N,N',N'*-tetraacetic acid, EGTA; 2-(*N*-morpholino)ethanesulphonic acid, MES; tetraethylammonium, TEA; *N*-methylglucamine, NMG; *N*-(2-hydroxyethyl)piperazine-*N'*-(2-ethanesulphonic acid), HEPES; 4-aminopyridine, 4-AP). This is similar to solutions used to induce 'blebbing' in skeletal muscle (Standen, Stanfield, Ward & Wilson, 1984).

Large-scale (20–50  $\mu\text{m}$ ) membrane bleb formation and/or apparent lifting of sarcolemma away from myofilaments were routinely found after 4–6 h incubation at 4 °C. As suggested by our micrographs (see Appendix), this process appeared to involve a pinching off of T-tubules from surface membrane, and it could be accelerated by hypotonicity (20–50 %) of the storage solution. All experiments described in this article were performed with membrane taken from cells kept at 4 °C for 6–48 h. For seal formation, the storage solution was modified by 40% dilution with distilled water to enhance membrane separation from myofilaments and by addition of 5 mM- $\text{MgCl}_2$  to enhance seal formation. The blebbing of fully relaxed myocytes could be largely hindered or reversed by replacing potassium with sodium, lithium or caesium, as well as by replacing chloride with MES. These observations suggest that permeant ions (i.e. potassium and chloride) are essential for membrane blebbing of the type described in this study and that disruption of Donnan equilibrium and volume regulation is importantly involved in the membrane blebbing process. Confocal images and electron micrographs of myocytes employed are presented in the Appendix to this article.

### *Giant patch formation*

Electrodes with 14–24  $\mu\text{m}$  inner diameter tips were pulled from borosilicate glass pipettes (Drummond (USA) N51A; 2.0 mm o.d./1.6 mm i.d.), usually by a conventional double-pull technique. The use of relatively large-diameter, thin-walled glass was advantageous for obtaining large-diameter pipette tips with relatively steep descent at the tip. However, it is important to note for applications requiring fast voltage clamp that thick-walled aluminosilicate, Corning No. 7052 or other borosilicate pipette types could readily be employed. Light fire-polishing with just-visible effects on the tip favoured the spontaneous formation of inside-out patches upon membrane excision, rather than vesicles which had to be disrupted mechanically. Alternatively, electrodes were pulled to smaller diameters and then were bevelled on the edge of a soft glass bead to the diameter desired. When such electrodes were employed without fire-polishing, the membrane generally remained localized immediately at the electrode opening during sealing, and vesicles were obtained in the great majority of cases upon membrane excision. As a third possible electrode preparation (which was found to be advantageous for work with oocytes) electrodes were bevelled to 40–60  $\mu\text{m}$  diameter and were melted to the diameter desired (18–40  $\mu\text{m}$ ) at a close distance from a glass bead on the microforge. The resulting pipette tips have a very steep descent which is advantageous for fast voltage clamping and pipette perfusion experiments. However, success rate in obtaining stable excised patches from cardiac myocytes was low.

A number of hydrocarbon mixtures consisting of oils, waxes and Parafilm allowed large-diameter, high-resistance seal formation. Several oils could be used by simply dipping the dry electrode tip into the oil of choice and then washing with the desired filling solution. From the different oils tested, best success was obtained with acetyltocopherol (Sigma; USA). Silicone oils and plasticizers were not useful. Importantly, the stability of seals formed with oils alone (particularly mineral oils) was rather limited both with respect to time and tolerance of voltage pulses.

The most consistent improvement of stability was obtained with a highly viscous mixture of Parafilm, acetyltocopherol or light mineral oil, and medical grade heavy mineral oil. The mixture was prepared by vigorously stirring over gas heat roughly three parts by weight of finely shredded Parafilm with one part each of the two oils for 30–60 min. Usually, acetyltocopherol could be used without mineral oil. A peanut-sized amount of the mixture was rubbed with a plastic rod on a clean surface, and a thin film of the mixture was drawn into air on the rod (see Fig. 1A). The electrode tip was then passed quickly through the film, and the procedure was repeated once. To reduce capacitance of the electrode, a thick coating of the mixture was applied to within about 100  $\mu\text{m}$  of the tip by rotating the electrode in a more thickly drawn film. Electrodes were backfilled and a brief, strong, positive pressure pulse was applied via a syringe to clear the tip. The immediate electrode tip then appeared clean and was visually indistinguishable from that of an untreated electrode.

Seals were formed by gentle negative pressure at the membrane surface, and membrane patches were excised. Patch resistances during experiments, using 14–24  $\mu\text{m}$  diameter electrode tips, ranged from 1 to 10 G $\Omega$ .

### *Recording chamber*

After excision, patches were moved into a plastic chamber system, which allowed rapid solution changes at the cytoplasmic membrane surface. The chamber is represented schematically in Fig. 1B. The polyethylene solution lines (0.25 mm i.d.) and the pipette tip chamber itself (1.2 mm inner diameter) were water-jacketed. Flow rate had no effect on temperature in the chamber or currents recorded. The solution lines exited to the electrode chamber (volume, 10–15  $\mu\text{l}$ ) via a  $\theta$ -style glass pipette (0.6 mm diameter). Solution changes were made to > 90% completion within 0.2 s by applying a pulse of pressure to the desired solution line with input syringe. A slow flow of solution through the desired solution line was maintained throughout all records presented. For more rapid solution changes, continuous solution flow was maintained through both lines, and the interface between the two solutions was moved across the patch. This could be carried out by a solenoid-controlled movement of the superfusion chamber or by rapid movement of the microscope stage.

In many experiments it was important to switch consecutively between different sets of solutions or use multiple solutions. To do so, one or both of the solution lines was cleared through the patch chamber after changing syringes to the desired new solutions. Solution changes made by flushing

solution lines ('slow solution switches') were 80% complete in less than 2 s.  $\text{MgATP}$  and chymotrypsin were routinely applied in this manner. Unless otherwise indicated, breaks in the data records presented correspond to time periods when this procedure was carried out to subsequently allow the desired rapid solution changes.

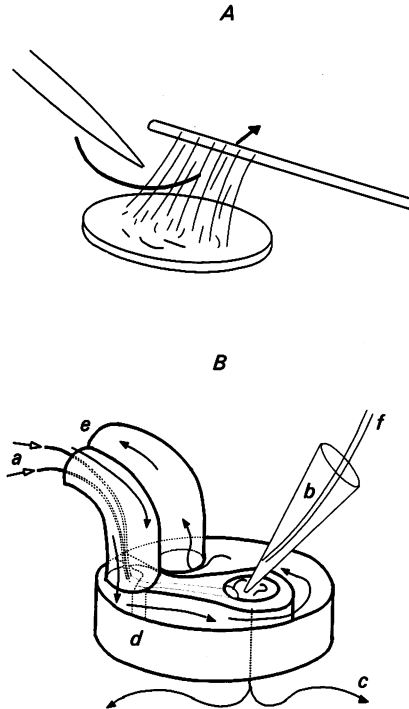


Fig. 1. *A*, method of application of viscous Parafilm-mineral oil-tocopherol mixture to pipette tip. A rod is rubbed longitudinally in a small amount of the hydrocarbon mixture and drawn into air. The electrode tip is passed through when a thin, homogeneous film is obtained, and the procedure is repeated once. *B*, diagram of temperature-controlled solution switcher used in experiments. Solution is pressed from syringes (not shown) through two polyethylene tubes (*a*, see open arrowheads; 0.25 mm i.d./0.6 mm o.d.), which have been pulled to a tip (approx. 0.1 mm i.d.) and glued into a  $\theta$ -style double-barrelled pipette with outlet in the actual superfusion chamber (1.2 mm diameter). Patches are excised in a relatively full Petri dish, and the pipette tip (*b*) is moved into the chamber. Subsequently, solution level in the Petri dish is lowered to approximately 1 mm depth. Solution level remains high in the pipette chamber, owing to water adhesion to the walls, and superfusion solution empties downward onto the floor of Petri dishes employed (*c*). The pipette chamber is surrounded by a plastic water jacket (*d*) with flow as indicated by arrows to the outlet (*e*). Pipette perfusion (*f*) has been carried out via the method of Soejima & Noma (1984). Temperature in the pipette chamber remains constant during pulsatile flow, and solution changes upon applying pressure to one or the other of the inflow syringes are 90% complete in approximately 0.2 s.

Membrane vesicles rather than inside-out patches were often formed during membrane excision, as indicated by an absence of  $\text{Na}^+ - \text{Ca}^{2+}$  exchange current in the present work. Vesicles could sometimes be disrupted by application of rapid solution pulses, whereby the sudden development of  $\text{Na}^+ - \text{Ca}^{2+}$  exchange current (or  $\text{Na}^+ - \text{K}^+$  pump current or  $\text{Na}^+$  currents) indicated success. More reliably, vesicles could be disrupted by touching the tip of the pipette against an air bubble or a

bead of hydrocarbon on the wall of the patch chamber. About 5% of total vesicles obtained broke to an outside-out configuration as evidenced by the  $\text{Na}^+$ - $\text{Ca}^{2+}$  exchange current characteristics obtained. Although membrane position in the pipette tip could often be well visualized, membrane patches could not be visually distinguished from vesicles.

All experiments reported in this article were carried out at 34–36 °C. Membrane potential was held at 0 mV using an Axopatch (USA) IC or Warner (USA) PC-501 patch clamp. Current changes were recorded directly onto chart paper (12 Hz response), and figures were prepared from current records after careful reproduction with a digitizing tablet. Leak currents were not subtracted. Capacitance of patches employed in this study was determined as described previously (Hilgemann, 1989) and ranged from 3 to 9 pF.

#### *Solutions and reagents for outward $\text{Na}^+$ - $\text{Ca}^{2+}$ exchange current measurements*

Magnesium adenosine triphosphate (MgATP), 1-(5-isoquinoline sulphonyl)-2-methylpiperazine (H7), cyclic AMP-dependent protein kinase inhibitor (synthetic: rabbit sequence), type IV-S acid phosphatase, and type 1-S chymotrypsin were purchased from Sigma (USA). Adenosine 5'-O-(3-thiotriphosphate) (ATP- $\gamma$ -S) and alkaline phosphatase were purchased from Boehringer Mannheim (FRG) and kindly donated by Dr James T. Stull (Department of Physiology, University of Texas Southwestern Medical Center). Type 2A cardiac phosphatase was a generous gift of Dr Marc C. Mumby (Department of Pharmacology, University of Texas Southwestern Medical Center). The peptide inhibitor of calcium-calmodulin-dependent protein kinase II (CaM kinase II) was kindly provided by Dr Howard Schulman (Department of Pharmacology, Stanford University, Palo Alto, CA, USA). The protein kinase C inhibitory peptide was synthesized at this institution (University of Texas Southwestern Medical Center). The calmodulin inhibitor peptide was a kind gift of Dr James T. Stull.

The patch electrodes contained (mM): 10 TEA, 20 CsCl, 0.5 BaCl<sub>2</sub>, 100 NMG, 100 MES, 20 HEPES, 2 MgCl<sub>2</sub>, 5 CaCl<sub>2</sub>, 10 LiCl (except for the experiment in Fig. 12, which had KCl instead of LiCl); and ( $\mu\text{M}$ ): 20 ouabain, 2 verapamil and 30 EGTA. The pH was adjusted to 7.0 with NMG or MES. Potassium was originally included in the electrode solution in light of a report of its stimulatory effect on  $\text{Na}^+$ - $\text{Ca}^{2+}$  exchange (Coutinho, Carvalho & Carvalho, 1983). Lithium was later substituted for potassium with no apparent change of results. Other similar experiments were conducted without MgCl<sub>2</sub> in the electrode with no apparent differences in results. With 20 mM-TEA and 1  $\mu\text{M}$ -glybenclamide in the electrode, omission of CsCl also had no apparent effects on currents recorded.

The superfusion solutions contained (in mM): 18 TEA, 18 CsCl, 18 HEPES, 1 MgCl<sub>2</sub>, 9 EGTA, 7 CaCl<sub>2</sub> (giving a free  $\text{Ca}^{2+}$  concentration of 1  $\mu\text{M}$ ), and 90 or 100 total additional NaCl or CsCl. The pH was adjusted to 7.0 with NMG. Some experiments were performed with all chloride in the superfusion solutions replaced with MES (e.g. Figs 5–7, 11 and 13B) or using lithium substitution for sodium instead of caesium (e.g. Fig. 12) with no apparent differences in results obtained. In all figures, '0 Na' denotes 90 or 100 mM-CsCl or CsMES unless otherwise indicated. MgATP and MgATP- $\gamma$ -S were added to the superfusion solutions in the form of a stock solution containing (mM): 50 or 100 MgATP, 5 or 10 MgCl<sub>2</sub>, 25 HEPES, pH adjusted to 7.0 with NMG. Solutions containing MgATP therefore contained an excess of Mg over ATP. '2 mM-MgATP' in figures refers to 2 mM-ATP plus 2.2 mM-total Mg.

## RESULTS

### *Validation of methods: $\text{Na}^+$ - $\text{K}^+$ pump current measurements*

The identification of well-characterized electrogenic mechanisms other than  $\text{Na}^+$ - $\text{Ca}^{2+}$  exchange is one possible way to validate the giant patch as a model of cardiac sarcolemma. Measurements of sodium current in giant cardiac patches have been described previously (Hilgemann, 1989). Basic measurements of sodium pump current in Figs 2 and 3 document rigorous control of cytoplasmic substrate concentrations and ion gradients, relevant to experiments presented subsequently on the  $\text{Na}^+$ - $\text{Ca}^{2+}$  exchange. To measure  $\text{Na}^+$ - $\text{K}^+$  pump current, ouabain and calcium were omitted from the pipette solution, and 10 mM-EGTA was included with

5 mM-KCl. A steady-state outward current of 5–30 pA was then routinely activated by the simultaneous application of both sodium and MgATP on the cytoplasmic side of patches, 16–22  $\mu\text{m}$  in diameter, excised from guinea-pig myocytes. This current was entirely absent when 0.25 mM-ouabain was included in the pipette. As shown in

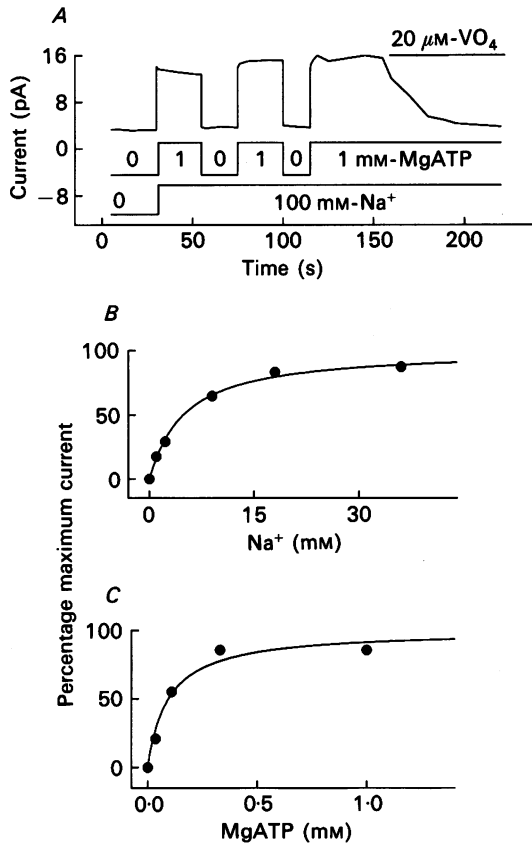


Fig. 2.  $\text{Na}^+-\text{K}^+$  pump current in excised giant guinea-pig cardiac sarcolemmal membrane patch. *A*, the pipette solution has no calcium, 10 mM-EGTA and 5 mM-KCl. As indicated, 100 mM-sodium was first applied together with 1 mM-MgATP by a slow solution switch. MgATP was then removed and reapplied as indicated in the presence of sodium, and finally 20  $\mu\text{M}$ -vanadate was applied in the presence of both MgATP and sodium. Results were indistinguishable when 5 mM-nickel or 1 mM-cadmium was included in the pipette with no EGTA. Results are typical for more than twenty observations. *B*, sodium dependence of  $\text{Na}^+-\text{K}^+$  pump current, fitted to a Hill equation. The  $K_d$  is 4.4 mM, and the slope is 1.06. *C*, MgATP dependence of  $\text{Na}^+-\text{K}^+$  pump current, fitted to a Michaelis-Menten equation. The  $K_d$  is 0.94 mM.

Fig. 2*A*, the current was completely inhibited by 20  $\mu\text{M}$ -vanadate on the cytoplasmic side.

The  $\text{Na}^+-\text{K}^+$  pump current was activated within solution switch times upon addition of MgATP and turned off within switch times upon removal of MgATP. The half-maximal MgATP concentration was 94  $\mu\text{M}$  (Fig. 2*C*), which corresponds well to

results with reconstituted  $\text{Na}^+\text{-K}^+$  pump (e.g. Goldshlegger, Karlish, Rephaeli & Stein, 1987). Activation by cytoplasmic sodium (Fig. 2A) was also immediate and was not accompanied by current transients. As in  $\text{Na}^+\text{-K}^+$  pump measurements by others (Nakao & Gadsby, 1985) under similar conditions, the sodium concentration

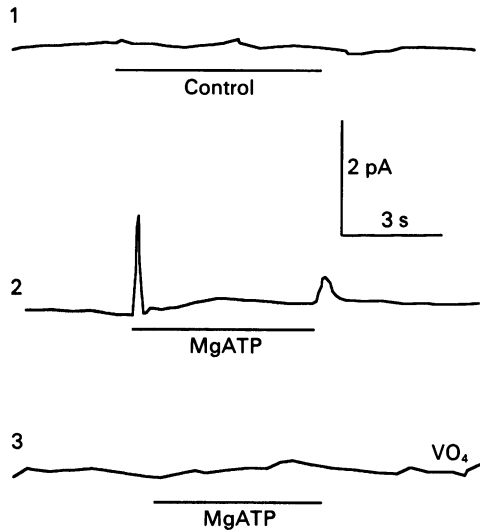


Fig. 3.  $\text{Na}^+\text{-K}^+$  pump charge movement resolved via MgATP concentration jumps in a giant guinea-pig cardiac sarcolemmal membrane patch (five similar experiments). The solutions given in Methods were modified as follows. The extracellular solution contains 10 mM-extracellular EGTA, 10 mM-extracellular sodium, no other extracellular monovalent cation, and no ouabain. The cytoplasmic solution is the usual 90 mM-caesium-containing solution with 10 mM-sodium. Record 1, control switch between solutions of the same composition. Record 2, current transient induced by application of 1 mM-MgATP. Record 3, same as record 2 with 100  $\mu\text{M}$ -vanadate added to the cytoplasmic solutions. Transients were absent when 0.25 mM-ouabain was included in the pipette (three patches).

dependence under these conditions was not steep. It was half-maximal at 4.4 mM. These results demonstrate immediate access of solutions to the cytoplasmic membrane surface and the lack of current transients in a mechanism other than  $\text{Na}^+\text{-Ca}^{2+}$  exchange which transports sodium.

As shown in Fig. 3, the control of solution composition and the speed of solution changes was adequate to resolve partial electrogenic reactions of the  $\text{Na}^+\text{-K}^+$  pump (e.g. Forbush, 1984; Nakao & Gadsby, 1986) via MgATP concentration jumps. To do so, extracellular (pipette) and cytoplasmic (superfusion) solutions contained 10 mM-sodium and the extracellular solution contained no potassium or caesium. A single cycle of sodium translocation was initiated by rapidly applying 1 mM-MgATP to the cytoplasmic side of the patch. Record 1 shows that 'sham' solution switches were free of electrical artifacts. Record 2 of Fig. 3 shows a typical outward current transient obtained when 1 mM-MgATP was rapidly applied. The peak of ATP-induced current was routinely 1–3 pA, and the transient was completed in about 0.2 s. The time course probably represents MgATP diffusion to the membrane

surface. As anticipated for the  $\text{Na}^+-\text{K}^+$  pump, application of MgATP did not cause a charge movement when cytoplasmic sodium was omitted or when 0.2 mM-ouabain was included in the pipette (not shown). Also, the transients were abolished by 100  $\mu\text{M}$ -vanadate, a cytoplasmic inhibitor of  $\text{Na}^+-\text{K}^+$  ATPase (Fig. 3, record 3). Integration of ATP-induced current transients indicates pump densities of 1200–3200 per  $\mu\text{m}^2$  (ten measurements with membrane area estimated from both observed patch geometry and membrane capacitance). This was, on average, twofold higher than densities measured by others in whole guinea-pig myocytes (Nakao & Gadsby, 1986).

These experiments allowed important methodological controls for pipette contamination with storage solution. Half-activation of steady-state  $\text{Na}^+-\text{K}^+$  pump current occurs with about 200  $\mu\text{M}$ -external potassium (Nakao & Gadsby, 1989) and seals were made in the presence of 100 mM-KCl. Particularly when seal formation was slow, steady-state currents were indeed obtained in these experiments. As apparent from lack of steady-state pump current in these records, however, contamination of the pipette solution by the bath solution can be less than 0.2%.

#### *Time course of $I_{\text{NaCa}}$ stimulation by MgATP*

Figure 4 shows the usual effect of 2 mM-MgATP on outward  $I_{\text{NaCa}}$  and the time course of its reversal after removal of MgATP. This patch was taken from a shortened myocyte, presumed to be depleted of ATP. As indicated in the figure, 90 mM-cytoplasmic sodium was applied to activate outward current. The current decayed by more than 90% before the first application of 2 mM-MgATP, which increased the current from about 20 pA to more than 70 pA over 1.5 min. After removal of MgATP the current remained stimulated and could be turned off and on several times by change of the sodium concentration. To quantify reversal of the stimulatory effect, an exponential was fitted to data points towards the end of exchange current transients obtained in the presence of cytoplasmic sodium. The  $t_{50}$  here was 247 s, and in a series of similar experiments averaged  $185 \pm 76$  s (mean  $\pm$  s.d.,  $n = 6$ ). Finally in Fig. 4B, 2 mM-MgATP was again applied, and a second response was obtained. The second response was reduced both in size and rate from the first response.

#### *$K_d$ of initial rate of stimulatory effect is greater than 3 mM-MgATP*

It was not usually possible to determine the steady-state dependence of outward exchange current on MgATP concentration, because decay rates of the stimulatory effect were too slow in relation to the life-time of patches to allow accurate measurements of multiple points. However, it can be stated with confidence that the half-maximum MgATP concentration for steady-state current was usually in the range of 0.5–1 mM. In patches from both rabbit and guinea-pig myocytes, application of 0.25 mM-MgATP had little or no effect over 5–10 min, while application of 5 mM-MgATP after prolonged application of 2 mM-MgATP had small but significant effects (not shown).

The dependence of the onset rate of the stimulatory effect on MgATP concentration was determined as described in Fig. 5A, and the results are shown in Fig. 5B. Filled circles in Fig. 5B are values from patches excised from rabbit myocytes; squares are

from guinea-pig myocytes. As indicated in Fig. 5A, cytoplasmic sodium was initially applied to activate an exchange current transient, and then a randomly chosen MgATP concentration from 0.1 to 5 mM was applied. Two minutes later 5 mM-MgATP was applied to all patches. The steepest slope of the rise of outward current

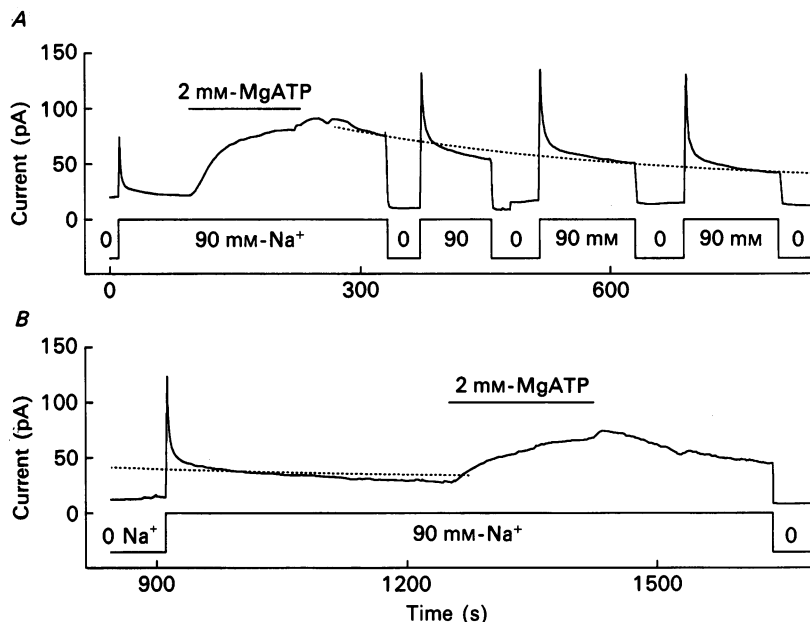


Fig. 4. Repetitive stimulation of Na<sup>+</sup>-Ca<sup>2+</sup> exchange current by MgATP in a patch from a guinea-pig myocyte. Note slow reversal. The bars above the current trace indicate the times during which the bath solution contained MgATP. The steps below the current trace indicate the concentration of Na<sup>+</sup> in the bath solution. The dashed line represents an exponential decay with a  $t_{50}$  of 247 s. Stimulation of exchange current by MgATP with slow reversal was observed in more than forty patches from guinea-pig and in eight patches from rabbit. Repetitive stimulation by MgATP with slow reversal was observed in thirteen patches.

during application of the test concentration of MgATP was determined over a 4 s period, and this slope was divided by the total current change with 5 mM-MgATP (i.e. current magnitude in 5 mM-MgATP minus current magnitude before application of the test concentration) to correct for surface area differences between patches. As apparent in Fig. 5B, the onset rate of the stimulatory effect continued to increase from 0.1 to 5 mM-MgATP. Results from rabbit patches were best fitted by a least-squares method to a Michaelis-Menten equation with a  $K_d$  of 12 mM. Note that the results at low MgATP concentrations show some sigmoidicity, which fits with our observation in other experiments that application of 0.1–0.4 mM-MgATP often had no effect on exchange current.

#### *The stimulatory effect can decay rapidly*

In patches from individual batches of both guinea-pig and rabbit myocytes, the

stimulatory effect of MgATP decayed on a time scale of seconds rather than many minutes. An example from guinea-pig sarcolemma is shown in Fig. 6 with a decay  $t_{50}$  of 20 s. This rapidly decaying effect of MgATP does not represent  $\text{Na}^+-\text{K}^+$  pump current since it was found to be insensitive to up to 1 mM-vanadate (three patches),

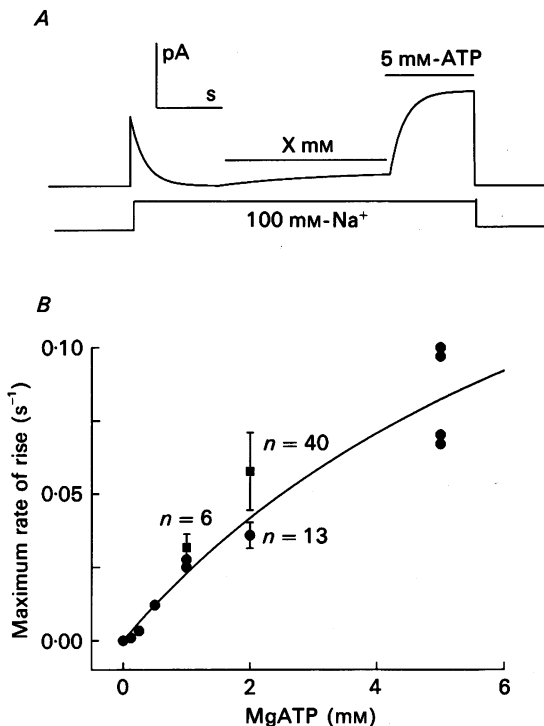


Fig. 5. Dependence of exchange current stimulation on MgATP concentration. All of the patches represented in this figure exhibited slow reversal of the MgATP effect. *A*, experimental protocol. Various concentrations of MgATP were applied to patches and the maximum rate of rise of the current was determined by drawing a tangent to the current trace by eye. This rate was divided by the maximum effect in 5 mM-MgATP to yield a rate expressed as the fraction of maximum effect per second. *B*, dependence of maximum rate of rise on MgATP concentration. Filled circles represent patches from rabbit myocytes; filled squares represent patches from guinea-pig myocytes. The curve is a Michaelis-Menten equation with a  $K_m$  of 12 mM, fitted to the rabbit data by a least-squares method. Error bars are  $\pm$  s.e.m.

and did not activate and deactivate within the time span of solution switches (compare Figs 2 and 6). Vanadate also had no effect on the rate of decay (three patches). Particularly in rabbit sarcolemmal patches, this response could be reproduced many times. With repeated applications over 20 min the response diminished by 30–60%. In guinea-pig patches, the MgATP response consistently diminished more markedly with repeated applications. The dependence of steady-state outward  $\text{Na}^+-\text{Ca}^{2+}$  exchange current on MgATP from a guinea-pig sarcolemmal patch is given in Fig. 7. The  $K_d$  for MgATP was 7.5 mM. The MgATP dependence of initial rates (not shown) was very similar to the steady-state MgATP dependence of

the current and to the MgATP dependence of initial rates in patches with slow decay. Reversal rates as high as  $0.3 \text{ s}^{-1}$  were obtained for the MgATP effect. In such patches the effect of MgATP consistently had a correspondingly rapid onset and was small in magnitude.

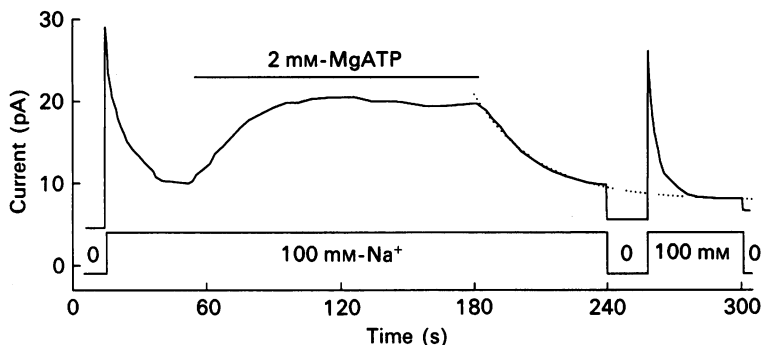


Fig. 6. Stimulation of exchange current by MgATP in a patch from a guinea-pig myocyte with rapid reversal of the MgATP effect. The dotted line represents an exponential decay with a  $t_{50}$  of 20 s. Rapid reversal of the MgATP effect was observed in ten patches from guinea-pig and in fifteen patches from rabbit.

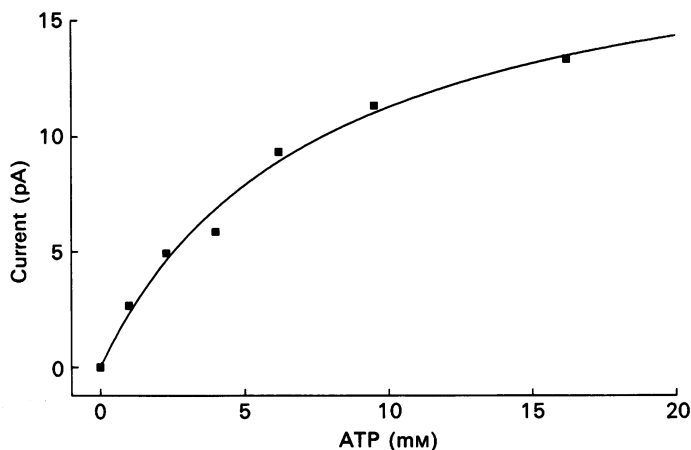


Fig. 7. Dependence of exchange current stimulation on MgATP concentration. Data from one patch (guinea-pig myocyte) with rapid reversal of the MgATP effect ( $t_{50} = 6 \text{ s}$ ). Data points represent the steady-state current in the presence of MgATP, minus the current in the absence of MgATP. The curve represents Michaelis-Menten concentration dependence with a  $K_d$  of  $7.5 \text{ mM}$ , fitted to the data points by a least-squares method. Similar data obtained from a second guinea-pig myocyte patch were fitted with a  $K_d$  of  $10.1 \text{ mM}$  (not shown).

The pharmacological experiments described subsequently have all been carried out in patches with the usual slow decay. Most pharmacological experiments have additionally been carried out in patches with fast decay, and results were very similar. Specifically, similar experiments have been carried out in both types of patches with vanadate (five patches with slow decay; three

patches with rapid decay), MgATP- $\gamma$ -S (five patches with slow decay; six patches with rapid decay), H7 (two patches with slow decay; two patches with rapid decay), and a protein kinase C inhibitory peptide (two patches with slow decay; one patch with rapid decay). Experiments with okadaic acid were carried out only in patches with fast decay. No qualitative differences have arisen to date between results with fast and slow decay. It was noteworthy, however, in patches with rapid decay rates that a slowly decaying component was sometimes also present (not shown), raising the possibility of two mechanisms. Our attempts to identify critical factors in obtaining patches with rapidly or slowly decaying stimulatory effects have been unsuccessful to date. Those attempts have included changes of all chemicals employed, cell isolations with five different collagenases, changes of animal strains employed, changes in the hydrocarbon mixtures employed for patch formation, and changes in the methods of seal formation and vesicle disruption.

*Onset of the stimulatory effect is not  $\text{Ca}^{2+}$  dependent*

Figure 8 demonstrates that the stimulatory effect of MgATP does not require cytoplasmic free calcium. In the first part of the record, outward exchange current was activated in the presence of  $1\ \mu\text{M}$ -free calcium. The patch was then superfused with calcium-free cytoplasmic solution with a small decrease of current. The leak current in  $90\ \text{mM}$ - $\text{Na}^+$  and zero calcium (9 pA) was less than that in  $90\ \text{mM}$ -caesium (11 pA), which is very probably due to the higher mobility of caesium in solution and therefore greater caesium leak current. Addition of  $2\ \text{mM}$ -MgATP to the superfusion solution at 350 s, in the zero-calcium solution, increased the current by 6 pA. Note that the time course of this small effect was very similar to the time course of MgATP action in normal cytoplasmic solution. The MgATP was then removed in the continued absence of free calcium. Subsequent superfusion with the calcium-containing solution at 570 s revealed a steady-state current of 40 pA greater than the caesium leak. Switching to caesium/no-sodium solution revealed that the current was entirely sodium sensitive, and the next switch from caesium to sodium at 670 s produced an exchange current with a peak of 70 pA above baseline and a steady state of 45 pA above baseline. A second MgATP application, this time in the presence of internal  $\text{Ca}^{2+}$ , had a small stimulatory effect, increasing the current by 15 pA. Since the second MgATP application came after a 4 min period of ATP-free superfusion, a 20% decay of the previous MgATP effect would entirely account for the second effect and could be expected (see e.g. reversal of MgATP effect in Fig. 4).

*MgATP reduces  $\text{Na}^+$ -dependent inactivation of  $I_{\text{NaCa}}$*

One consistent effect of MgATP application was a reduction of the current decay phase upon application of cytoplasmic sodium. As shown in Fig. 9, MgATP sometimes had little effect on peak currents obtained while nearly abolishing the transient phase. The small increase of the baseline outward current in this record corresponds to a decrease of the seal resistance, which could occur at any time. In more than fifty observations, MgATP always reduced the fraction of  $\text{Na}^+-\text{Ca}^{2+}$  exchange current which decayed during application of sodium. As described previously (Hilgemann, 1990), an increase of cytoplasmic calcium also reduced the transient phase in such experiments. This suggests that there might be a common mechanistic end-point of the two actions.

*MgATP shifts secondary  $\text{Ca}^{2+}$  dependence of  $I_{\text{NaCa}}$  to the left*

Such a mechanistic link between the effects of calcium and MgATP is demonstrated

in Fig. 10. Figure 10A shows the effect of MgATP on the steady-state dependence of outward  $\text{Na}^+$ - $\text{Ca}^{2+}$  exchange current on cytoplasmic calcium. Circles are results from a patch with slow decay of the stimulatory effect of MgATP. Squares are results from a patch with fast decay of the stimulatory effect. As verified in more than ten

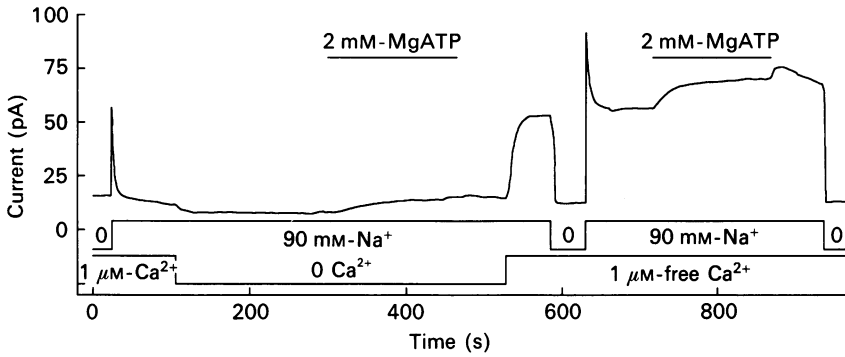


Fig. 8. Stimulation of  $\text{Na}^+$ - $\text{Ca}^{2+}$  exchange current by MgATP in the absence of internal calcium (guinea-pig myocyte patch). The steps below the current trace indicate the concentrations of sodium and free calcium in the superfusion solution. Similar results were obtained in three patches.

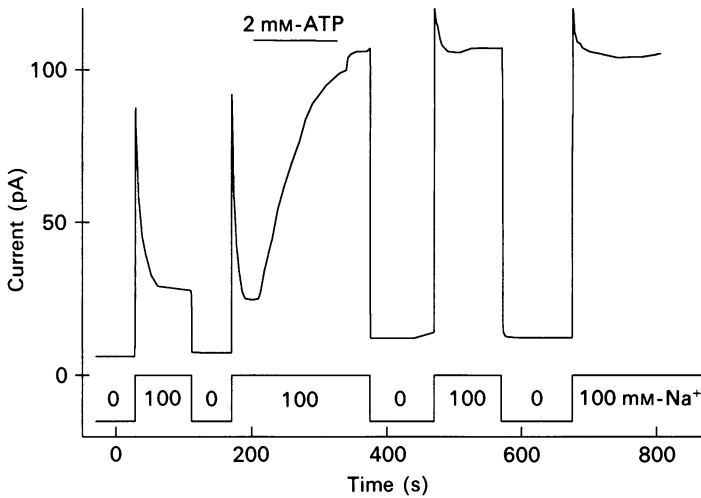


Fig. 9. MgATP-induced reduction of outward exchange current decay (inactivation) during application of  $\text{Na}^+$  (guinea-pig myocyte patch). As indicated, 100 mM- $\text{Na}^+$  was applied repetitively. During the second application, 2 mM-MgATP was additionally applied for 110 s. Note that current decays by > 70% during  $\text{Na}^+$  application before MgATP. Peak current remains increased after MgATP by about 15%, and the decay of current upon application of sodium is almost eliminated.

experiments, the secondary calcium dependence of outward  $\text{Na}^+$ - $\text{Ca}^{2+}$  exchange current was shifted by a good log unit to higher calcium concentrations in patches with rapid decay of the stimulatory effect compared with patches with slow decay.

In both types of patches, results obtained with 4 mM-MgATP (filled symbols) were shifted to the left from results before addition of MgATP (open symbols). All results were fitted to a Michaelis-Menten equation. For all results, free calcium concentrations were checked with a calcium electrode. Nearly identical results were

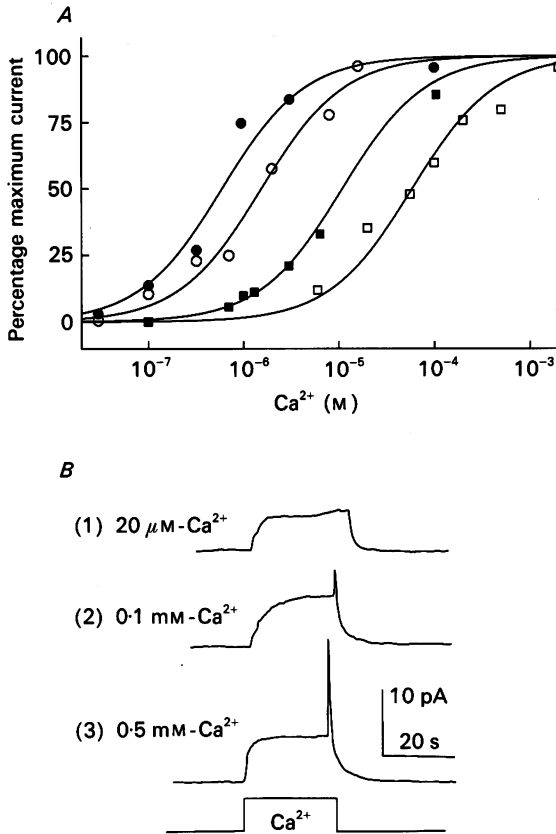


Fig. 10. MgATP-induced shifts of the secondary dependence of outward exchange current on cytoplasmic free calcium (guinea-pig myocyte patches). *A*, open symbols are before application MgATP. Filled symbols are with 4 mM-MgATP. Squares are from a patch with rapid reversal of the MgATP effect (two complete experiments, > 10 patches studied without MgATP); circles are from a patch with slow decay of the MgATP effect (two complete experiments, > 10 patches studied without MgATP). *B*, method of determining concentration dependence with cytoplasmic calcium concentrations >  $10 \mu\text{M}$ . As indicated, the cytoplasmic calcium concentration was jumped from zero to the desired value and back to zero. The direct inhibitory effect of cytoplasmic calcium on the calcium influx exchange cycle is released immediately, while the secondary activation decays slowly, giving rise to current transients as shown. Peak values in zero calcium were assumed to accurately reflect the calcium dependence of secondary activation.

obtained in patches with  $K_d$  values greater than  $50 \mu\text{M}$  when solutions were used without calcium buffering (not shown).

A complication in the results of Fig. 10*A* was that free cytoplasmic calcium directly inhibited the outward exchange current at concentrations greater than

about  $50 \mu\text{M}$ . Figure 10B shows how this complication was avoided in obtaining the data in Fig. 10A. Free calcium was always increased from zero to the desired concentration and decreased again back to zero. Importantly, decay of the secondary activation by calcium takes seconds in zero-calcium solution, while the direct

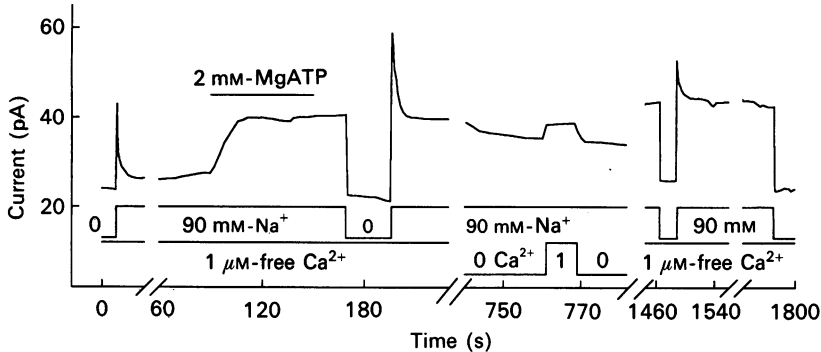


Fig. 11. Stimulation of exchange current by MgATP in a patch from a mouse myocyte. Changes in sodium and free calcium concentrations in the superfusion solution are indicated below the current trace. During the first break in the record a second transient was activated. The last break was included to help illustrate that the MgATP effect was sustained for almost 30 min. Stimulation of exchange current by MgATP was observed in seven patches from mouse myocytes.

inhibitory effect of cytoplasmic calcium is immediate. For this reason, there was a fast increment of the current upon removing high calcium concentrations. The peak values obtained immediately upon calcium removal were assumed to reflect the true secondary dependence of current on calcium concentration.

In eight similar experiments, data were fitted to Hill equations, and the Hill coefficients obtained in the absence of MgATP ranged from 0.73 to 1.2, giving no evidence for co-operativity in the activating effect of calcium. In the presence of MgATP, however, variable results were obtained. When  $K_d$  values for calcium were less than  $1 \mu\text{M}$ , higher Hill coefficients were obtained. For the filled circles in Fig. 10, for example, a Hill coefficient of 1.6 was obtained. Hill coefficients of up to 3.05 were obtained in highly stable patches when  $K_d$  values for calcium were  $0.4\text{--}0.8 \mu\text{M}$ . These were the lowest  $K_d$  values obtained in excised patches.

#### *MgATP can remove secondary $\text{Ca}^{2+}$ dependence of $I_{\text{NaCa}}$*

Application of MgATP usually induced a small calcium-insensitive component of outward exchange current in both guinea-pig and rabbit cardiac patches. This is apparent in Fig. 8 during application of MgATP in the absence of calcium and is also apparent in previously published results (Hilgemann, 1990). As shown in Fig. 11, the calcium-insensitive component was much larger in patches from mouse myocytes (four observations). Before application of MgATP, exchange current in patches from mouse myocytes was inhibited by at least 85% upon removal of cytoplasmic calcium (not shown). After application of MgATP, calcium removal inhibited only 10–15% of the steady-state exchange current. Reversal of the MgATP effect in patches from mouse myocytes was negligible over patch lifetimes of more than 30 min.

*MgATP- $\gamma$ -S does not mimic the effects of MgATP*

Magnesium was found to be essential for the effect of ATP in cardiac sarcolemma, and other nucleotides (ADP, AMP, GTP and AMP-PNP) were without effect on the outward  $\text{Na}^+ - \text{Ca}^{2+}$  exchange current in concentrations up to 5 mM (not shown). In

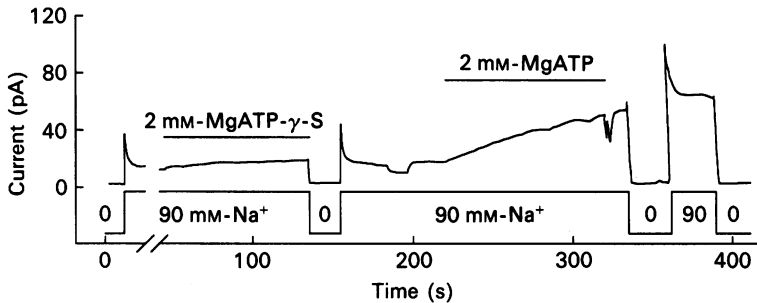


Fig. 12. The effect of  $\text{MgATP-}\gamma\text{-S}$  on  $\text{Na}^+ - \text{Ca}^{2+}$  exchange current (guinea-pig myocyte patch). '0  $\text{Na}^+$ ' indicates substitution of lithium for sodium. The inward deflection at 320 s is an artifact caused by the changing of superfusion solutions. Similar results were obtained in a total of five patches from guinea-pig with slow reversal of the  $\text{MgATP}$  effect, five patches from guinea-pig with rapid reversal, and one patch from rabbit with rapid reversal.

Fig. 12, the inability of  $\text{MgATP-}\gamma\text{-S}$  to mimic  $\text{MgATP}$  is described (ten similar experiments, with and without magnesium, and also with  $\text{MgATP-}\gamma\text{-S}$  application in the presence of 0.3 mM- $\text{MgATP}$ ).  $\text{ATP-}\gamma\text{-S}$  is regarded as being a relatively good substrate for protein kinases as opposed to ATPases (e.g. Gratecos & Fischer, 1974). From ten similar experiments, 2 mM- $\text{MgATP-}\gamma\text{-S}$  had an apparent effect only in the case shown in Fig. 12, increasing the steady-state exchange current by 4 pA (16%) and the peak by 12 pA (17%). This effect was small, however, compared to that of subsequently applying 2 mM- $\text{MgATP}$ , which increased the steady state by 40 pA (420%) and the peak by 50 pA (130%). Note that the rise of outward current with  $\text{MgATP}$  was rather slow. This was typical after prolonged exposures to  $\text{MgATP-}\gamma\text{-S}$ . Negative results were obtained with four different batches of  $\text{ATP-}\gamma\text{-S}$ , two of which had been bioassayed for activity with calcium-dependent protein kinases (Dr James T. Stull laboratory, University of Texas Southwestern Medical Center).

*Phosphatases and phosphatase inhibitors are without effect on stimulatory effect of MgATP*

If phosphoprotein phosphatases are involved in the reversal of the  $\text{MgATP}$  effect, inhibition of phosphatases would be expected to enhance the  $\text{MgATP}$  effect at intermediate  $\text{MgATP}$  concentrations and to slow the decay of the effect after removal of  $\text{MgATP}$ . Okadaic acid, a potent inhibitor of protein phosphatases type 1 and type 2A (Ishihara, Martin, Brautigam, Karaki, Ozaki, Kato, Fusetani, Watabe, Hashimoto, Uemura & Hartshorne, 1989), had no effect on the exchange current at a concentration of 2  $\mu\text{M}$  in the presence of 0.5 and 2 mM- $\text{MgATP}$  (two observations on patches with rapid decay). Also, 2  $\mu\text{M}$ -okadaic acid had no effect on the time course

of current decay upon removal of 10 mM-MgATP (comparison of decay time courses with repetitive applications of MgATP in a patch with rapid decay; one observation).

Alkaline phosphatase did not reverse the MgATP effect (three observations in patches with slow decay; not shown) at a concentration 15 times higher than

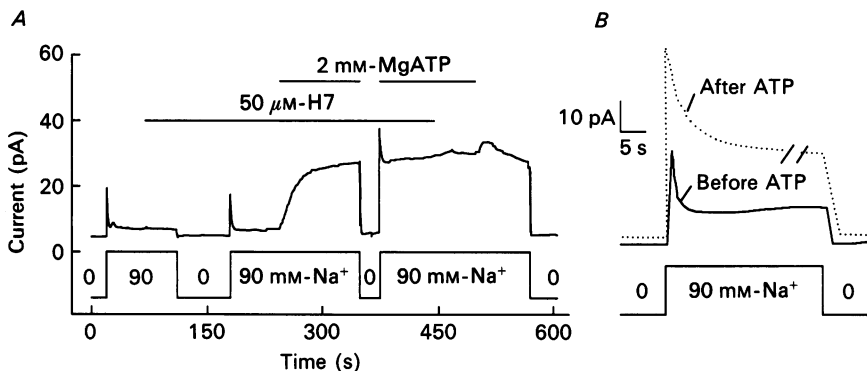


Fig. 13. Stimulation of  $\text{Na}^+-\text{Ca}^{2+}$  exchange current by MgATP in the presence of protein kinase inhibitors. *A*, MgATP applied in the presence of  $50 \mu\text{M}$ -H7 in the superfusion solution; patch from guinea-pig myocyte. *B*, stimulation of exchange current by MgATP in the presence of CaM kinase II inhibitor peptide; superimposed current transients from a patch taken from a mouse cardiac myocyte. The continuous line represents a transient recorded before application of peptide and MgATP. Forty-five seconds later  $10 \mu\text{M}$ -peptide was applied, followed by 2 mM-MgATP after a further 40 s, whereupon the current was stimulated in the continued presence of peptide. MgATP had no further effect upon removal of the peptide. The dotted line represents a transient recorded after MgATP was washed out. The break in the record was included to facilitate comparison of the two transients.

concentrations needed to reverse effects of exogenously added protein kinase A on channels in excised cardiac patches (Kim, 1990). Similarly, 4-8 units/ml acid phosphatase were without effect on the reversal of the stimulatory effect (three experiments; not shown). In addition to commercially available phosphatases, the ability of the catalytic subunit of a type 2A cardiac protein phosphatase (Mumby, Green & Russell, 1985) to reverse the effect of MgATP was tested in the three experiments. The isolated cardiac phosphatase was applied in concentrations known to rapidly dephosphorylate a variety of phosphoproteins. It was entirely without effect on the MgATP-stimulated outward exchange current (not shown).

#### *Protein kinase inhibitors do not block the effect of MgATP*

As shown in Fig. 13*A*, 2 mM-MgATP strongly and rapidly stimulated the exchange current in the presence of  $50 \mu\text{M}$  of the non-specific protein kinase inhibitor, H7 (Hidaka, Inagaki, Kawamoto & Sasaki, 1984) (three similar experiments). When added to the superfusion solutions, here at 70 s,  $50 \mu\text{M}$ -H7 alone had no effect on the exchange current. With H7 still present, 2 mM-MgATP increased the exchange current here by 24 pA. No further effect of MgATP was observed when H7 was removed. In a separate experiment, MgATP stimulated  $\text{Na}^+-\text{Ca}^{2+}$  exchange current in the presence of  $200 \mu\text{M}$ -H7.

Four peptide inhibitors of protein kinases have been tested as inhibitors of the stimulatory effect of MgATP. The effects were evaluated by comparing the magnitudes and rates of onset of the stimulatory effect of MgATP as in Fig. 4. The first peptide was the calmodulin inhibitor peptide, corresponding to the calmodulin binding sequence of myosin light chain kinase (Blumenthal, Takio, Edelman, Charbonneau, Titani, Walsh & Krebs, 1985). This peptide strongly inhibited outward exchange current in the absence of MgATP in the concentration range of 0.2–2  $\mu\text{M}$  (Hilgemann & Cash, 1990), and this result precluded further studies with respect to MgATP. Notably, the affinity of the block was only 2- to 4-fold lower than for 'exchange inhibitory peptide' (Li, Nicoll, Collins, Hilgemann, Filoteo, Penniston, Weiss, Tomich & Philipson, 1991). The second peptide was a protein kinase A inhibitor peptide (Sigma). The peptide had no effect on control exchange current or the stimulatory effect of MgATP at a concentration of 10  $\mu\text{M}$ . The third peptide was a C-kinase inhibitory peptide consisting of residues 19–31 of the pseudosubstrate domain of protein kinase C (Malinow, Schulman & Tsien, 1989). No effect of this peptide was obtained at concentrations of up to 6  $\mu\text{M}$  (three observations).

The fourth peptide was a CaM kinase II inhibitory peptide consisting of residues 273–302 of this kinase (Malinow *et al.* 1989) with a threonine substitution at position 286. From results like those shown in Fig. 13B, it is concluded that this peptide also had no significant effect on the stimulatory effect of MgATP at concentrations up to 15  $\mu\text{M}$ . Figure 13B shows current transients obtained in a mouse patch before and after MgATP, applied in the presence of the peptide.

#### DISCUSSION

The results presented establish for the first time that the  $\text{Na}^+-\text{Ca}^{2+}$  exchange system of cardiac cells is modulated by MgATP concentration changes in the range of several millimolar. The strikingly low affinity for MgATP distinguishes the underlying mechanism from most, if not all, known protein kinases and ATPases. Furthermore, the low affinity of the process for MgATP raises the possibility that the exchange process might be modulated by MgATP concentration changes taking place physiologically and/or pathologically.

Before discussing details of the findings, the giant patch method will be discussed in the light of data presented here and reported previously. Since the data were obtained on membrane blebs arising from the sarcolemma, bleb formation and the relevance of bleb membrane to normal physiological processes will also be discussed on the basis of micrographs presented in the Appendix to this article.

#### *Assessment of the giant cardiac membrane patch method*

In giant excised cardiac membrane patches, the densities of sodium channel current (Hilgemann, 1989), sodium pump current (Hilgemann, Nagel & Gadsby, 1991), sodium pump charge movement (this article), and  $\text{Na}^+-\text{Ca}^{2+}$  exchange current (Hilgemann, 1989) are within a factor of approximately two from those determined in whole-cell measurements. Sodium current behaves in excised giant patches similarly to sodium current in conventional patches (e.g. Fernandez, Fox & Krasne, 1984) in that steady-state inactivation is shifted by approximately 30 mV towards

more negative potentials than in intact cells (Hilgemann, 1989). For the sodium pump, differences between the intact state and the excised or isolated state are not yet established, although it is striking that both current densities and charge movement densities described here are about twofold greater in giant patches than in whole myocytes. For the  $\text{Na}^+$ - $\text{Ca}^{2+}$  exchanger, the most striking difference established to date is that the secondary activation by cytoplasmic calcium is shifted by at least one log unit to higher free calcium concentrations from that described in intact myocytes. While it is tempting to suggest that these differences come about from a loss of diffusible cytoplasmic factors, this remains to be established firmly.

The micrographs in the Appendix show that neither T-tubules nor organelles (in particular sarcoplasmic reticulum) are associated with the bleb structures from which membrane is excised. It appears that surface membrane at first lifts away from myofilaments along each sarcomere, while remaining attached at Z-lines (lower edge of Fig. 14). Then, membrane progressively detaches at Z-lines, the openings of T-tubules become pinched off, and the bleb structures merge along the surface of the myocyte. As shown in the micrographs, T-tubules directly beneath the blebs evidently remain in communication with the extracellular space, presumably via longitudinal T-tubules.

Membrane blebs can become impressively large on completely relaxed myocytes in relation to the relatively small foci from which they appear to sprout and in relation to the cylindrical surface dimensions of myocytes (e.g. 20  $\mu\text{m}$  diameter in Fig. 16, and up to 50  $\mu\text{m}$  in routine observations). The large dimensions raise an important question as to the origin of the bleb membrane. Two general possibilities are consistent with results up to now: (1) insertion of new membrane could be an important mechanism of bleb formation or enlargement, (2) infoldings of normal surface membrane, including surface caveolae, could constitute a larger source of membrane for bleb formation than generally expected from capacitance measurements. Although the capacitance of biological membranes is often assumed to be about 1  $\mu\text{F}/\text{cm}^2$ , lower values of 0.6–0.7  $\mu\text{F}/\text{cm}^2$  have been reported (Valdiosera, Clausen & Eisenberg, 1974). Also, the morphological quantification of surface *vs.* T-tubule membrane areas is not precise. Regardless of which possibility is more applicable, it has been firmly established that the bleb membrane contains normal sarcolemmal ion transport mechanisms in roughly the densities expected from whole-cell measurements.

Within the time resolution of solution switches, about 0.1 s, measurements of  $\text{Na}^+$ - $\text{K}^+$  pump activity and partial electrogenic reactions demonstrate that MgATP has free access to and away from the cytoplasmic membrane surface of giant patches. Within this same time frame, there is no indication for a restricted 'pool' of subsarcolemmal ATP. Furthermore, the close agreement between ATP dependencies of  $\text{Na}^+$ - $\text{K}^+$  pump current in giant patches and  $\text{Na}^+$ - $\text{K}^+$  pump activity in reconstituted systems gives no reason to suspect that ATP gradients develop at the membrane surface due to overall membrane ATPase activity. Accordingly, the concentration dependencies of the stimulatory effect of MgATP on outward  $\text{Na}^+$ - $\text{Ca}^{2+}$  exchange activity must be assumed to be accurate. In the specific case of cytoplasmic calcium changes, it is important that a direct inhibition of outward  $\text{Na}^+$ - $\text{Ca}^{2+}$  exchange current by high cytoplasmic calcium is relieved within the solution switch

time (Fig. 10B) upon reduction of cytoplasmic free calcium. Accordingly, it must be assumed that the measured secondary dependencies of outward  $\text{Na}^+-\text{Ca}^{2+}$  exchange current on cytoplasmic calcium are accurate, and that the relatively slow, multisecond time scale of secondary current activation by cytoplasmic calcium is also accurate.

*Secondary dependence of outward  $\text{Na}^+-\text{Ca}^{2+}$  exchange current on cytoplasmic MgATP*

That the secondary calcium dependence of  $\text{Na}^+-\text{Ca}^{2+}$  exchange does not involve MgATP, and therefore does not involve a phosphorylation mechanism, was a striking early finding with the giant patch method (Hilgemann, 1989). The present work provides the first demonstration that the calcium influx mode of  $\text{Na}^+-\text{Ca}^{2+}$  exchange can be strongly stimulated by MgATP in the complete absence of cytoplasmic calcium (Fig. 8), thereby completing the documentation of two separate mechanisms. Experiments of this kind were not possible in squid giant axons because of the relatively long times needed to change cytoplasmic solutions (10–15 min). Also, the present work provides the first measurements of the initial rate of onset of the stimulatory effect of MgATP (Fig. 5). The ability to perform this measurement is essential for studying the underlying mechanism, because steady-state measurements of ATP dependence reflect both the process responsible for generation of the effect and the process responsible for its decay. As expected for a simple system with an ATP-dependent onset and an ATP-independent decay rate, the ATP dependence of the steady state when decay of the stimulatory effect is rapid nearly matches the ATP dependence of the initial rate (Figs 5 and 7).

On the basis of the present work, the involvement of any of the well-characterized serine protein kinases must be regarded as highly unlikely. First, the non-specific kinase inhibitor, H7, and three peptide inhibitors of serine protein kinases did not inhibit the stimulatory effect of MgATP. Second, the MgATP concentration dependence of onset of the stimulatory effect is inconsistent with any of the well-characterized serine or tyrosine kinases, which are fully activated at submillimolar concentrations of MgATP (e.g. Morris & Khan, 1986; Edelman, Blumenthal & Krebs, 1987). Third, MgATP- $\gamma$ -S did not substitute for MgATP in stimulating  $\text{Na}^+-\text{Ca}^{2+}$  exchange current, whereas it can act as a substrate for some protein kinases (e.g. Gratecos & Fischer, 1974). Fourth, three different phosphoprotein phosphatases were without effect on the reversal of the stimulatory effect. It is unlikely that the lack of effect of these enzymes was due to restricted access to the membrane surface, since the  $\text{Na}^+-\text{Ca}^{2+}$  exchange current in excised patches was strongly stimulated by phospholipase D (Hilgemann & Collins, 1992). Fifth, the phosphatase inhibitor, okadaic acid, was without effect on the MgATP effect and its decay. Obviously, this work does not rule out the possibility of  $\text{Na}^+-\text{Ca}^{2+}$  exchange regulation in intact cells by one of the well-characterized protein kinases.

On the basis of the present work three functional effects of MgATP on outward  $\text{Na}^+-\text{Ca}^{2+}$  exchange current have been distinguished: a reduction of the extent of current decay (inactivation) during application of cytoplasmic sodium, an increased sensitivity to cytoplasmic calcium in secondary exchange activation, and the development of calcium-independent current. Of these three, it has been notable that the development of calcium-independent exchange current, in contrast to the other

effects, has never been observed to reverse with time after removal of MgATP. Possible mechanisms for this effect must therefore include the dissociation of a regulatory factor or a MgATP-stimulated proteolysis (DeMartino, McGuire & Croall, 1988).

*Relationship of secondary activation by cytoplasmic calcium to the effect of MgATP*

The main functional effects of MgATP in giant patches correlate very well with effects found in squid axon. First, MgATP in the squid axon stimulates the exchanger only (or primarily) in the presence of cytoplasmic sodium, leading to a conclusion that MgATP releases inhibition by cytoplasmic sodium (Requena, 1978). The parallel in the present study is that MgATP reduces the transient portion of outward exchange current during application of cytoplasmic sodium. Second, MgATP in the squid axon shifts the cytoplasmic calcium dependence of the calcium influx exchange mode to lower free calcium concentrations (Blaustein, 1977), just as described in Fig. 10 for the giant patch. Third, the steady-state MgATP dependence of exchanger-mediated calcium influx in the giant axon is half-maximum at about 0.5 nM. This fits reasonably to our estimates of the MgATP dependence of exchange current in patches with slow reversal of the MgATP effect.

These functional observations all appear consistent with a common mechanism. Strikingly, however, in the squid axon ATP- $\gamma$ -S potently stimulates Na<sup>+</sup>-Ca<sup>2+</sup> exchange (DiPolo & Beaugé, 1987*a, b*) and Ca<sup>2+</sup>-Ca<sup>2+</sup> exchange (Blaustein, 1977; DiPolo & Beaugé, 1990), while it is without effect on Na<sup>+</sup>-Ca<sup>2+</sup> exchange current in giant patches or even inhibits the subsequent stimulatory effect of MgATP (Fig. 12). In addition, the enhancement by vanadate of ATP-stimulated Na<sup>+</sup>-Ca<sup>2+</sup> exchange in squid axon (DiPolo & Beaugé, 1981) and ferret erythrocytes (Frame & Milanick, 1990) has not been observed in cardiac sarcolemmal patches. For the time being, the only available explanation of these disparate results is that different or additional mechanisms underlie the effects in the squid giant axon.

That the secondary cytoplasmic calcium dependence of outward Na<sup>+</sup>-Ca<sup>2+</sup> exchange current can shift by at least two orders of magnitude is a very striking but, at present, enigmatic finding. Given the fact that half-activation of outward exchange current in intact myocytes takes place at 30–70 nM free cytoplasmic calcium (Kimura *et al.* 1987; Noda, Shepherd & Gadsby, 1988; Miura & Kimura, 1989), the total possible concentration shift of secondary activation spans three full log units. That the effect of MgATP is intimately linked to the secondary activation by calcium is indicated not only by the shifts obtained with MgATP, but also by the fact that calcium dependence is shifted to the range of 0.1 nM when the decay of the stimulatory effect of MgATP is fast.

Three possible explanations for changes of calcium sensitivity with application of MgATP can be suggested. The calcium binding site(s) involved in the secondary activation by calcium could have a very low calcium affinity, and MgATP could act on reactions subsequent to occupation of binding site(s). Secondly, the availability of binding sites for occupation by calcium could be variable, and MgATP could act by favouring their availability and therefore their apparent affinity. As a third possibility, MgATP could increase the actual affinity of the binding sites for calcium. These possibilities, and the variability of Hill coefficients obtained for the secondary activation by calcium, all indicate the need for further experimental work.

We are grateful to Dr Christiane M. Baud for many helpful suggestions and to Dr David C. Gadsby for his encouragement and discussions. We also thank Mr David Cash and Mr Henry Liao for excellent technical assistance. This work was supported by an Established Investigatorship and a Grant-in-Aid from the American Heart Association and by a New Investigatorship of the NIH to D. W. H.

REFERENCES

- BAKER, P. F. & McNAUGHTON, P. A. (1976). Kinetics and energetics of calcium efflux from intact squid giant axons. *Journal of Physiology* **259**, 103–144.
- BARCENAS-RUIZ, L., BEUCKELMANN, D. J. & WEIR, W. G. (1987). Sodium–calcium exchange in heart: Membrane current and changes in  $[\text{Ca}^{++}]_i$ . *Science* **238**, 1720–1722.
- BAUMANN, O., KITAZAWA, T. & SOMLYO, A. P. (1990). Laser confocal scanning microscopy of the surface membrane/T-tubular system and the sarcoplasmic reticulum in insect striated muscle stained with  $\text{DiI-C}_{18}(3)$ . *Journal of Structural Biology* **105**, 154–161.
- BLAUSTEIN, M. P. (1977). Effects of internal and external cations and of ATP on sodium–calcium and calcium–calcium exchange in squid axons. *Biophysical Journal* **20**, 79–111.
- BLUMENTHAL, D. K., TAKIO, K., EDELMAN, A. M., CHARBONNEAU, H., TITANI, K., WALSH, K. A. & KREBS, E. G. (1985). Identification of the calmodulin-binding domain of skeletal muscle myosin light chain kinase. *Proceedings of the National Academy of Sciences of the USA* **82**, 3187–3191.
- CAMPBELL, D. L., GILES, W. R. & ROBINSON, K. (1988). Studies of sodium–calcium exchange in bull-frog atrial myocytes. *Journal of Physiology* **403**, 317–340.
- CARONI, P. & CARAFOLI, E. (1983). The regulation of the Na/Ca exchanger of heart sarcolemma. *European Journal of Biochemistry* **132**, 451–460.
- COUTINHO, O. P., CARVALHO, A. P. & CARVALHO, C. A. M. (1983). Effect of monovalent cations on Na/Ca exchange and ATP-dependent Ca transport in synaptic plasma membranes. *Journal of Neurochemistry* **41**, 670–676.
- CRESPO, L. M., GRANTHAM, C. J. & CANNELL, M. B. (1990). Kinetics, stoichiometry and role of the Na–Ca exchange mechanism in isolated cardiac myocytes. *Nature* **345**, 618–621.
- DEMARTINO, G. N., MCGUIRE, M. J. & CROALL, D. E. (1988). Ubiquitin-mediated and ubiquitin-independent pathways of intracellular proteolysis. In *Current Communications in Molecular Biology: The Ubiquitin System*, ed. SCHLESINGER, M. & HERSHKO, A., pp. 126–129. Cold Spring Harbor Laboratory.
- DIPOLLO, R. & BEAUGÉ, L. (1981). The effects of vanadate on calcium transport in dialyzed squid axons: sidedness of vanadate–cation interactions. *Biochimica et Biophysica Acta* **645**, 229–236.
- DIPOLLO, R. & BEAUGÉ, L. (1987a). In squid axons, ATP modulates Na–Ca exchange by a  $\text{Ca}_i$ -dependent phosphorylation. *Biochimica et Biophysica Acta* **897**, 347–354.
- DIPOLLO, R. & BEAUGÉ, L. (1987b). Characterization of the reverse Na/Ca exchange in squid axons and its modulation by  $\text{Ca}_i$  and ATP. *Journal of General Physiology* **90**, 505–525.
- DIPOLLO, R. & BEAUGÉ, L. (1988). Ca transport in nerve fibers. *Biochimica et Biophysica Acta* **947**, 549–569.
- DIPOLLO, R. & BEAUGÉ, L. (1990). Assymmetrical properties of the Na–Ca exchanger in voltage-clamped, internally-dialyzed squid axons under symmetrical ionic conditions. *Journal of General Physiology* **95**, 819–835.
- EARM, Y. E., HO, W. K. & SO, I. S. (1989). An inward current activated during late low-level plateau phase of the action potential in rabbit atrial cells. *Journal of Physiology* **410**, 64P.
- EDELMAN, A. M., BLUMENTHAL, D. K. & KREBS, E. G. (1987). Protein serine/threonine kinases. *Annual Review of Biochemistry* **56**, 567–613.
- EGAN, T. M., NOBLE, D. & NOBLE, S. (1989). Sodium–calcium exchange during the action potential in guinea-pig ventricular cells. *Journal of Physiology* **411**, 639–661.
- FEDIDA, D., NOBLE, D. & SHIMONI, Y. (1987). Inward currents and contraction in guinea-pig ventricular myocytes. *Journal of Physiology* **385**, 565–589.
- FERNANDEZ, J. M., FOX, A. P. & KRASNE, S. (1984). Membrane patches and whole-cell membranes: A comparison of electrical properties in rat clonal pituitary ( $\text{GH}_3$ ) cells. *Journal of Physiology* **356**, 565–586.
- FORBUSH, B. III (1984). Rapid ion movements in a single turnover of the  $\text{Na}^+$  pump. In *The*

- Sodium Pump: 4th International Conference on Na, K-ATPase*, ed. GLYNN, I. M. & ELLORY, J. C., pp. 599–611. The Company of Biologists, Cambridge, UK.
- FRAME, M. D. & MILANICK, M. A. (1990). ATP increases Na/Ca and Na/Mn exchange in resealed ferret red blood cell ghosts. *Biophysical Journal* **57**, 180a.
- GOLDSHLEGGER, R., KARLISH, S. J. D., REPHAEI, A. & STEIN, W. D. (1987). The effect of membrane potential on the mammalian sodium–potassium pump reconstituted into phospholipid vesicles. *Journal of Physiology* **387**, 331–355.
- GRATECOS, D. & FISCHER, E. H. (1974). Adenosine 5'-O(3-thiotriphosphate) in the control of phosphorylase activity. *Biochemical and Biophysical Research Communications* **58**, 960–967.
- HAWORTH, R. A., GOKNUR, A. B., HUNTER, D. R., HEGGE, J. O. & BERKOFF, H. A. (1987). Inhibition of calcium influx in isolated adult rat heart cells by ATP depletion. *Circulation Research* **60**, 586–594.
- HIDAKA, H., INAGAKI, M., KAWAMOTO, S. & SASAKI, Y. (1984). Isoquinolinesulfonamides, novel and potent inhibitors of cyclic nucleotide dependent protein kinases and protein kinase C. *Biochemistry* **23**, 5036–5041.
- HILGEMANN, D. W. (1986). Extracellular calcium transients and action potential configuration changes related to post-stimulatory potentiation in rabbit atrium. *Journal of General Physiology* **87**, 675–706.
- HILGEMANN, D. W. (1989). Giant excised cardiac sarcolemmal membrane patches: Sodium and sodium–calcium exchange currents. *Pflügers Archiv* **415**, 247–249.
- HILGEMANN, D. W. (1990). Regulation and deregulation of cardiac Na–Ca exchange in giant excised sarcolemmal membrane patches. *Nature* **344**, 242–245.
- HILGEMANN, D. W. & CASH, D. P. (1990). Secondary modulation of outward Na/Ca exchange current in giant excised cardiac sarcolemmal membrane patches. *Biophysical Journal* **57**, 308a.
- HILGEMANN, D. W. & COLLINS, A. (1992). Mechanism of cardiac Na<sup>+</sup>–Ca<sup>2+</sup> exchange current stimulation by MgATP: possible involvement of aminophospholipid translocase. *Journal of Physiology* **454**, 59–82.
- HILGEMANN, D. W., NAGEL, G. A. & GADSBY, D. C. (1991). Na/K<sup>+</sup> pump current in giant membrane patches excised from ventricular myocytes. In *The Sodium Pump: Recent Developments*, ed. DEWEER, P. & KAPLAN, J. H., pp. 543–547. Rockefeller University Press, New York.
- HILGEMANN, D. W. & NOBLE, D. (1987). Excitation–contraction coupling and extracellular calcium transients in rabbit atrium. *Proceedings of the Royal Society B* **230**, 163–205.
- HONG, M. G. & HUME, R. I. (1989). DiI and DiO: Versatile fluorescent dyes for neuronal labelling and pathway tracing. *Trends in Neurosciences* **12**, 331–341.
- ISHIHARA, H., MARTIN, B. L., BRAUTIGAN, D. L., KARAKI, H., OZAKI, H., KATO, Y., FUSETANI, N., WATABE, S., HASHIMOTO, K., UEMURA, D. & HARTSHORNE, D. J. (1989). Calyculin A and okadaic acid: Inhibitors of protein phosphatase activity. *Biochemical and Biophysical Research Communications* **159**, 871–877.
- KIM, D. (1990). Beta-adrenergic regulation of the muscarinic-gated K channel by cyclic AMP-dependent protein kinase in atrial cells. *Circulation Research* **67**, 1292–1298.
- KIMURA, J., MIYAMAE, S. & NOMA, A. (1987). Identification of sodium–calcium exchange current in single ventricular cells of guinea-pig. *Journal of Physiology* **384**, 199–222.
- KIMURA, J., NOMA, A. & IRISAWA, H. (1986). Sodium–calcium exchange current in mammalian heart cells. *Nature* **319**, 596–597.
- LI, Z., NICOLL, D. A., COLLINS, A., HILGEMANN, D. W., FILOTEO, A. G., PENNISTON, J. T., WEISS, J. N., TOMICH, J. M. & PHILIPSON, K. D. (1991). Identification of a peptide inhibitor of the cardiac sarcolemmal Na<sup>+</sup>–Ca<sup>2+</sup> exchanger. *Journal of Biological Chemistry* **266**, 1014–1020.
- MALINOW, R., SCHULMAN, H. & TSIEN, R. W. (1989). Inhibition of postsynaptic PKC or CaMKII blocks induction but not expression of LTP. *Science* **245**, 862–866.
- MIURA, Y. & KIMURA, J. (1989). Sodium–calcium exchange current: dependence on internal Ca and Na and competitive binding of external Na and Ca. *Journal of General Physiology* **93**, 1129–1148.
- MORRIS, F. W. & KAHN, C. R. (1986). The insulin receptor and tyrosine phosphorylation. In *The Enzymes*, ed. BOYER, P. D. & KREBS, E. G., vol. 27, pp. 247–305. Academic Press, New York.
- MUMBY, M. C., GREEN, D. D. & RUSSELL, K. L. (1985). Structural characterization of cardiac protein phosphatase with a monoclonal antibody. Evidence that the M<sub>r</sub> = 38,000 phosphatase is the catalytic subunit of the native enzyme(s). *Journal of Biological Chemistry* **260**, 13763–13770.

- NAKAO, M. & GADSBY, D. C. (1985). Nonlinear dependence of Na/K pump current on pipette  $[\text{Na}^+]$  in isolated heart cells. *Journal of General Physiology* **86**, 30a.
- NAKAO, M. & GADSBY, D. C. (1986). Voltage dependence of Na translocation by the Na/K pump. *Nature* **323**, 628–630.
- NAKAO, M. & GADSBY, D. C. (1989).  $[\text{Na}]$  and  $[\text{K}]$  dependence of the Na/K pump current–voltage relationship in guinea-pig ventricular myocytes. *Journal of General Physiology* **94**, 15.
- NELSON, M. T. & BLAUSTEIN, M. P. (1981). Effects of ATP and vanadate on calcium efflux from barnacle muscle fibres. *Nature* **289**, 314–316.
- NODA, M., SHEPHERD, N. & GADSBY, D. C. (1988). Activation by  $[\text{Ca}]_i$  and block by 3'4'-dichlorobenzamil, of outward Na/Ca exchange current in guinea-pig ventricular myocytes. *Biophysical Journal* **53**, 342a.
- REEVES, J. P. & PHILIPSON, K. D. (1989). Sodium–calcium exchange activity in plasma membrane vesicles. In *Sodium–Calcium Exchange*, ed. ALLEN, T. J., NOBLE, D. & REUTER, H., pp. 27–53. Oxford University Press, Oxford.
- REQUENA, J. (1978). Calcium efflux from squid axons under constant sodium electrochemical gradient. *Journal of General Physiology* **72**, 443–470.
- SHAO, Z., BAUMANN, O. & SOMLYO, A. P. (1991). Axial resolution of confocal microscopes with parallel-beam detection. *Journal of Microscopy* **164**, 13–19.
- SOEJIMA, M. & NOMA, A. (1984). Mode of regulation of the ACh-sensitive K-channel by the muscarinic receptor in rabbit atrial cells. *Pflügers Archiv* **400**, 424–431.
- STANDEN, N. B., STANFIELD, P. R., WARD, T. A. & WILSON, S. W. (1984). A new preparation for recording single-channel currents from skeletal muscle. *Proceedings of the Royal Society B* **221**, 455–464.
- TERASAKI, M., SONG, J., WONG, J. R., WEISS, M. J. & CHEN, L. B. (1984). Localization of endoplasmic reticulum in living and glutaraldehyde fixed cells with fluorescent dyes. *Cell* **38**, 101–108.
- VALDIOSERA, R., CLAUSEN, C. & EISENBERG, R. S. (1974). Impedance of frog skeletal muscle fibers in various solutions. *Journal of General Physiology* **63**, 460–491.

## APPENDIX

Fig. 14. Confocal image of a guinea-pig myocyte incubated in storage solution (see Methods) containing the carbocyanine dye DiI-C<sub>16</sub>-(3) (1,1'-dihexadecyl-3,3,3',3'-tetramethylindo-carbocyanineperchlorate; Honig & Hume, 1989; Baumann, Kitizawa & Somlyo, 1990). The cell was incubated for 10 min on ice in 10 µg/ml DiI, followed by rinsing in dye-free solution. The fibre was viewed with a 63× objective through rhodamine filters on a Bio-Rad 600 laser scanning confocal microscope fitted to a Zeiss Axiovert, and modified with a beam expander to improve axial resolution (Shao, Baumann & Somlyo, 1991). The dye incorporates into the plasma membrane, transverse tubule membranes and the intercalated disc region. The interior of the bleb is not stained. Note the punctate staining of the mouths of the transverse tubules (arrows) through the surface of the cell. Bar = 10 µm.

Fig. 15. A series of confocal images of a small membrane bleb on a rat myocyte stained with DiI-C<sub>16</sub>-(3) using procedures outlined in the legend to Fig. 14. A series of twenty images were collected at 0.36 µm steps. Panels A, B, C and D represent the 11th, 14th, 15th and 19th sections respectively. Note that the fluorescently stained transverse tubules do not extend into the membrane bleb. Bar = 6 µm.

Fig. 16. Paired images of a typical rat myocyte incubated in storage solution and DiOC<sub>6</sub>[3][3,3'-diagxyloxacarbo-cyanine iodide] which selectively stains mitochondria and the reticulum membranes (Terasaka, Song, Wong, Weiss & Chen, 1984). Myocytes were incubated for 20 min in 0.5 µg dye/ml storage solution, followed by several rinses of storage solution. Three large membrane blebs are visible in the transmitted image (B) but are barely discernible in the fluorescence image (A) indicating a lack of organelles within those regions. Bar = 25 µm.

Fig. 17. Electron micrograph of a portion of a typical rat myocyte with a large membrane bleb. The bleb has partially collapsed during the fixation and processing for electron microscopy. Bar = 5 µm.

Fig. 18. A higher magnification view of the membrane bleb shown in Fig. 17 illustrating the lack of organelles within the membrane bleb which contains only amorphous granular and filamentous osmiophilic material. The transverse tubules and junctional SR (arrows) remain close to the myofibrils. Bar = 1 µm. Inset, high magnification view of the outer aspect of a myocyte bleb showing a typical trilaminar membrane with osmiophilic filamentous material predominantly associated with the cytoplasmic face. Bar = 0.1 µm.

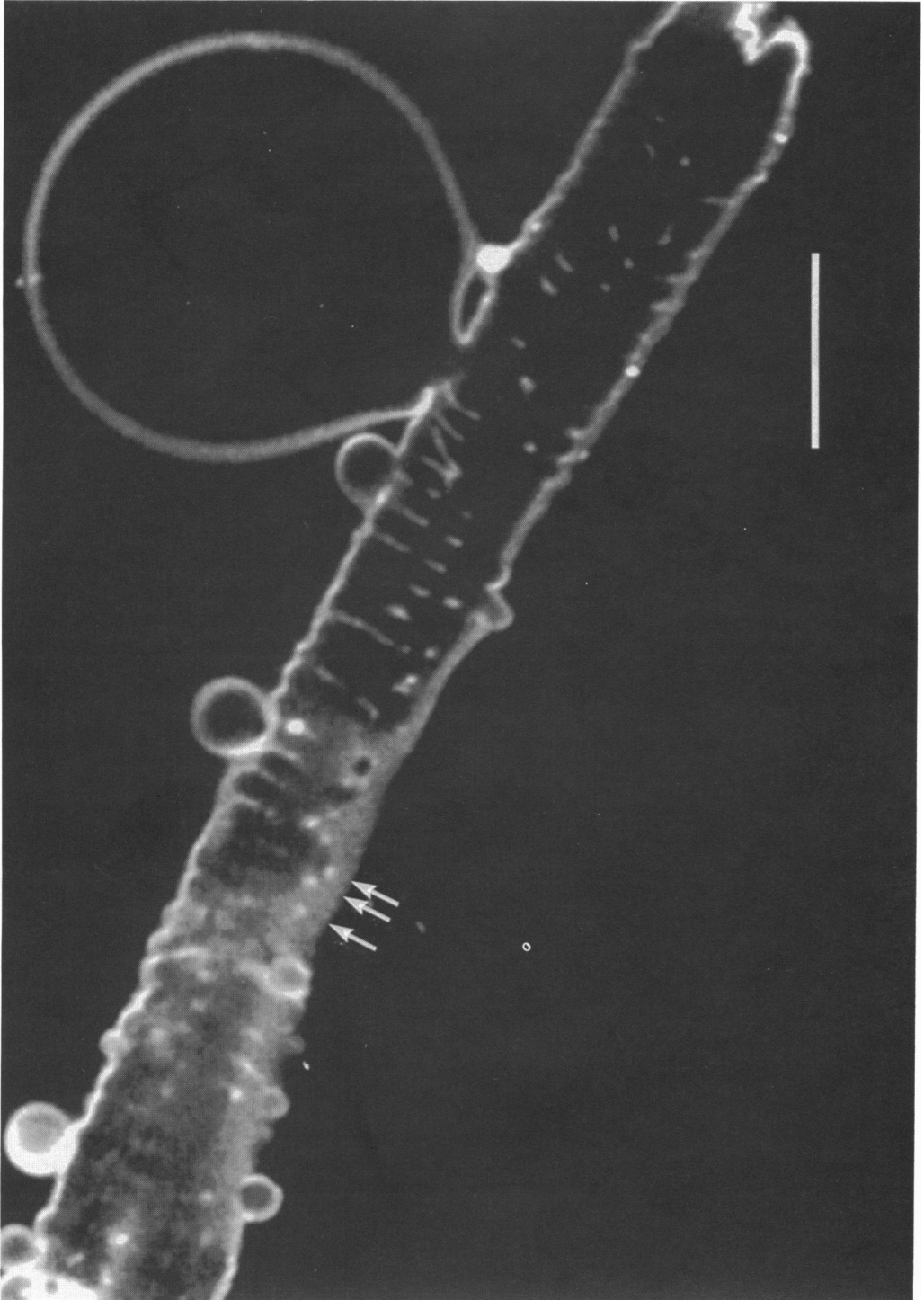


Fig. 14. For legend see facing page.

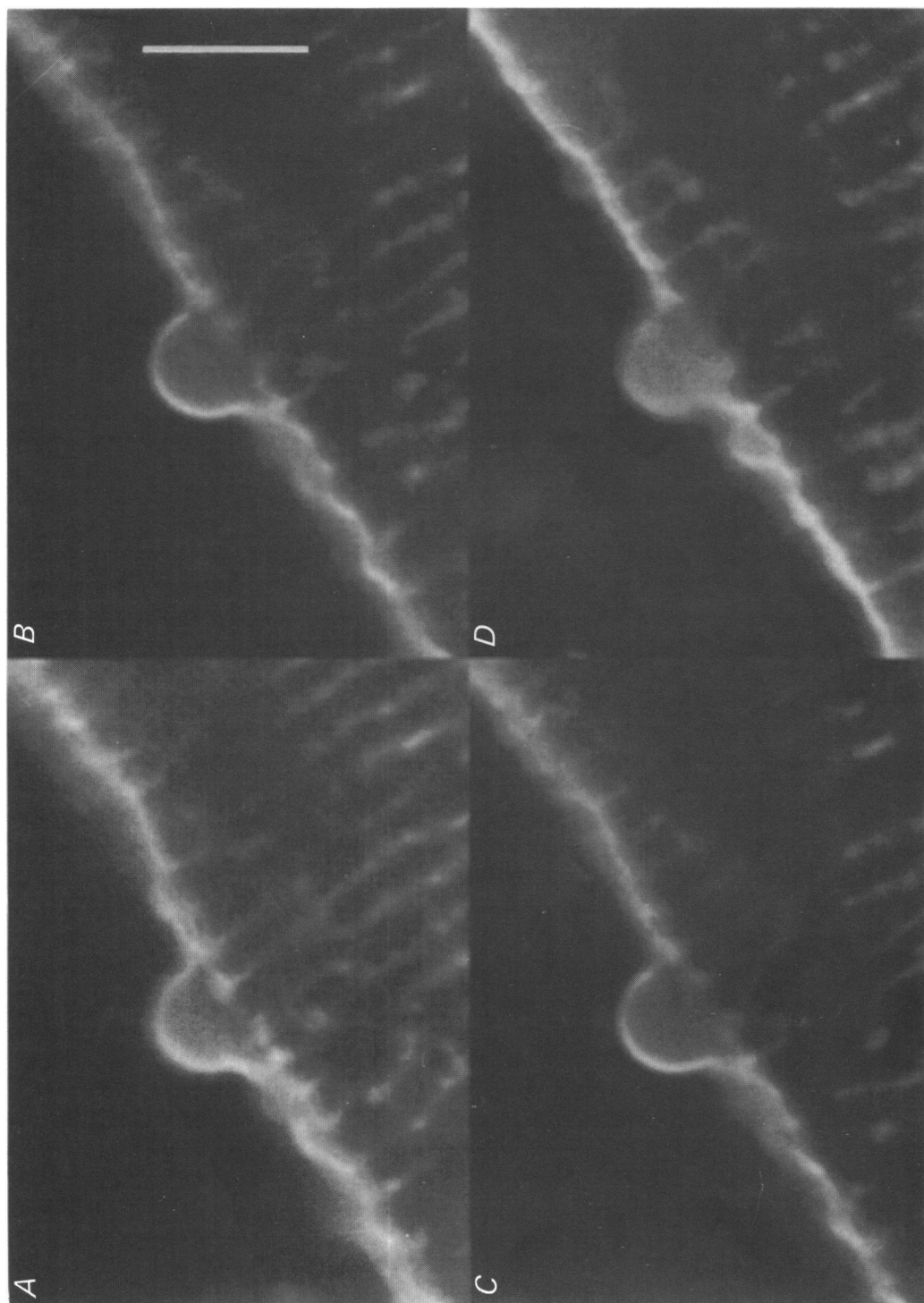


Fig. 15. For legend see page 52.

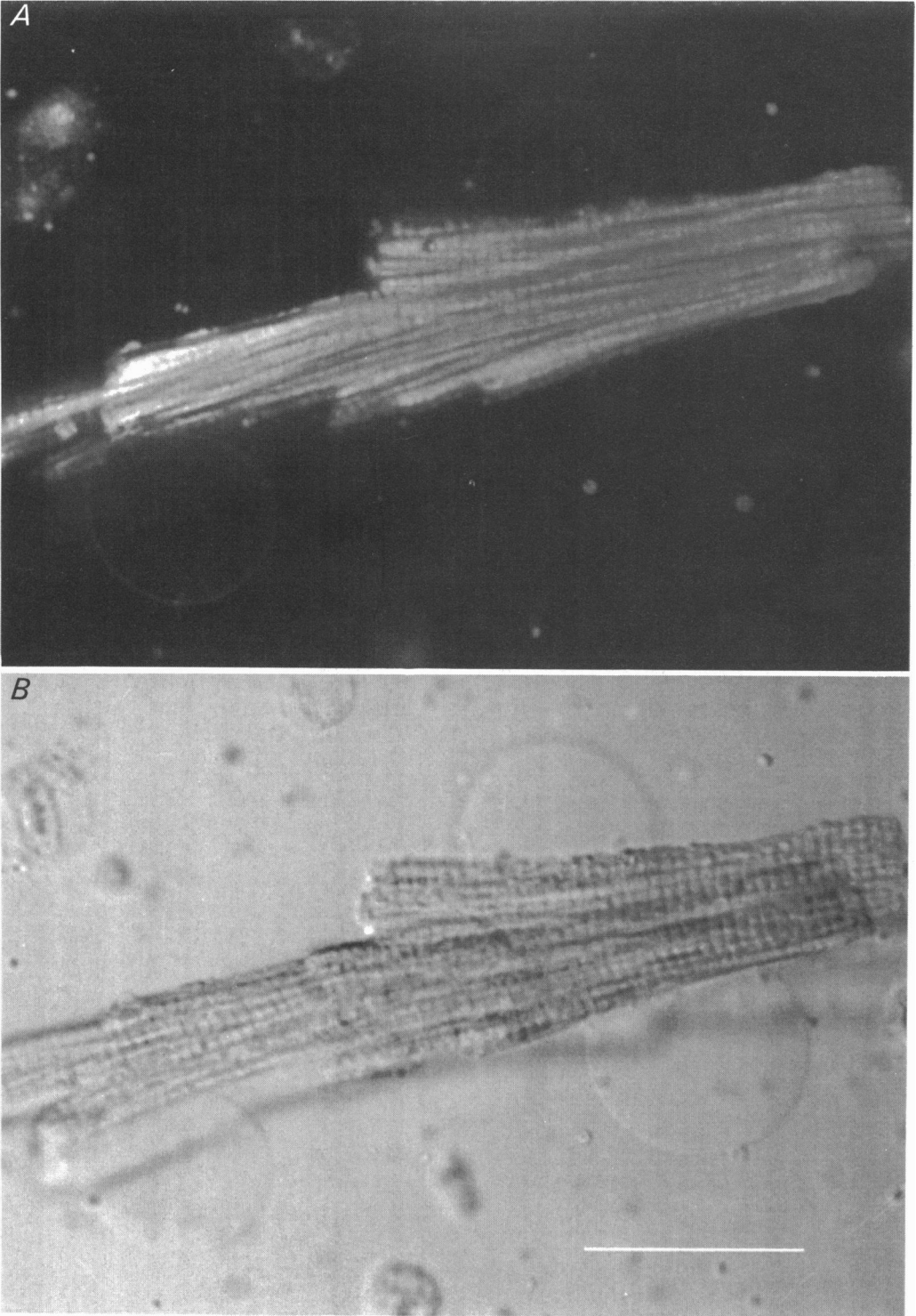


Fig. 16. For legend see page 52.

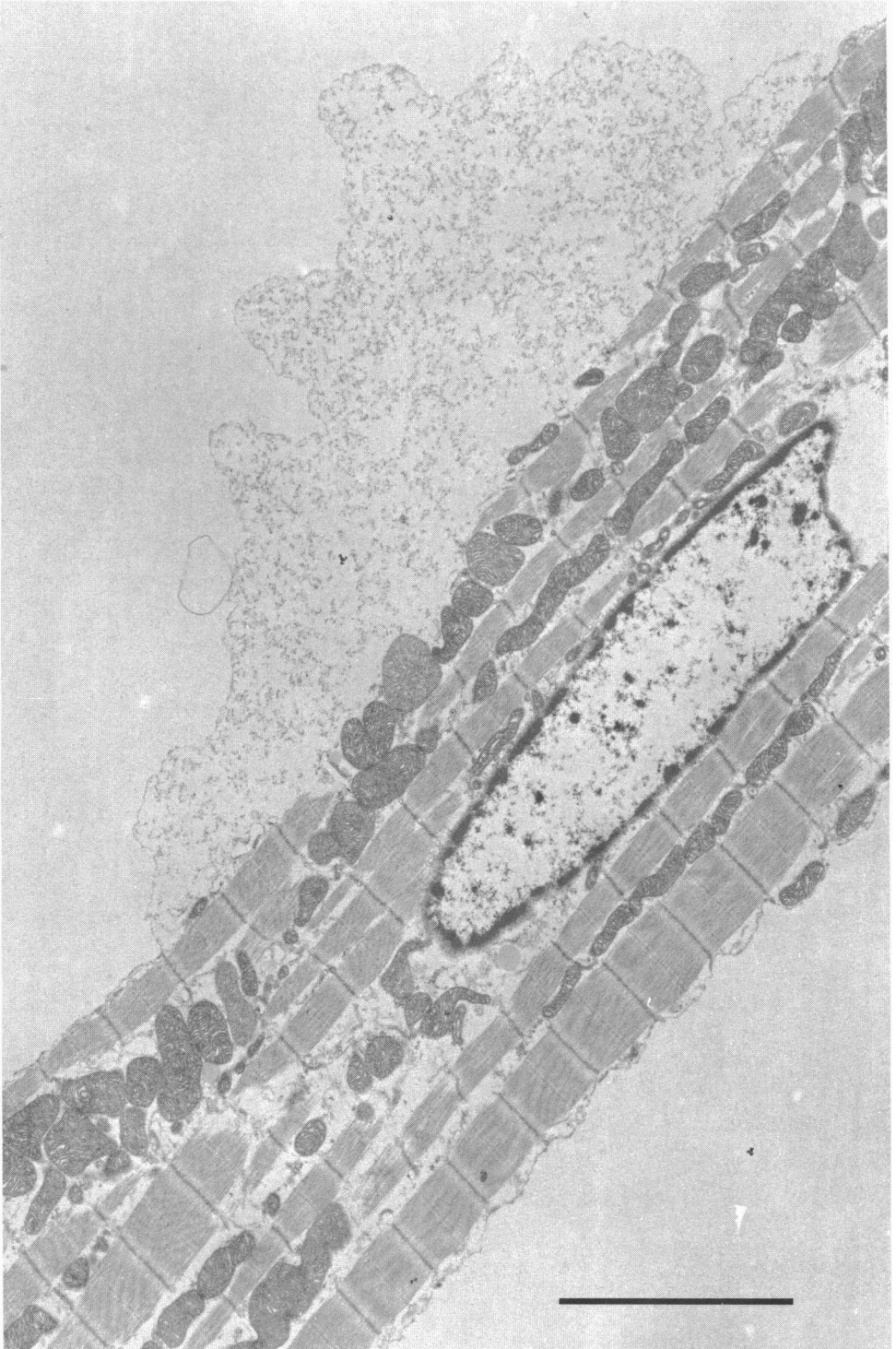


Fig. 17. For legend see page 52.

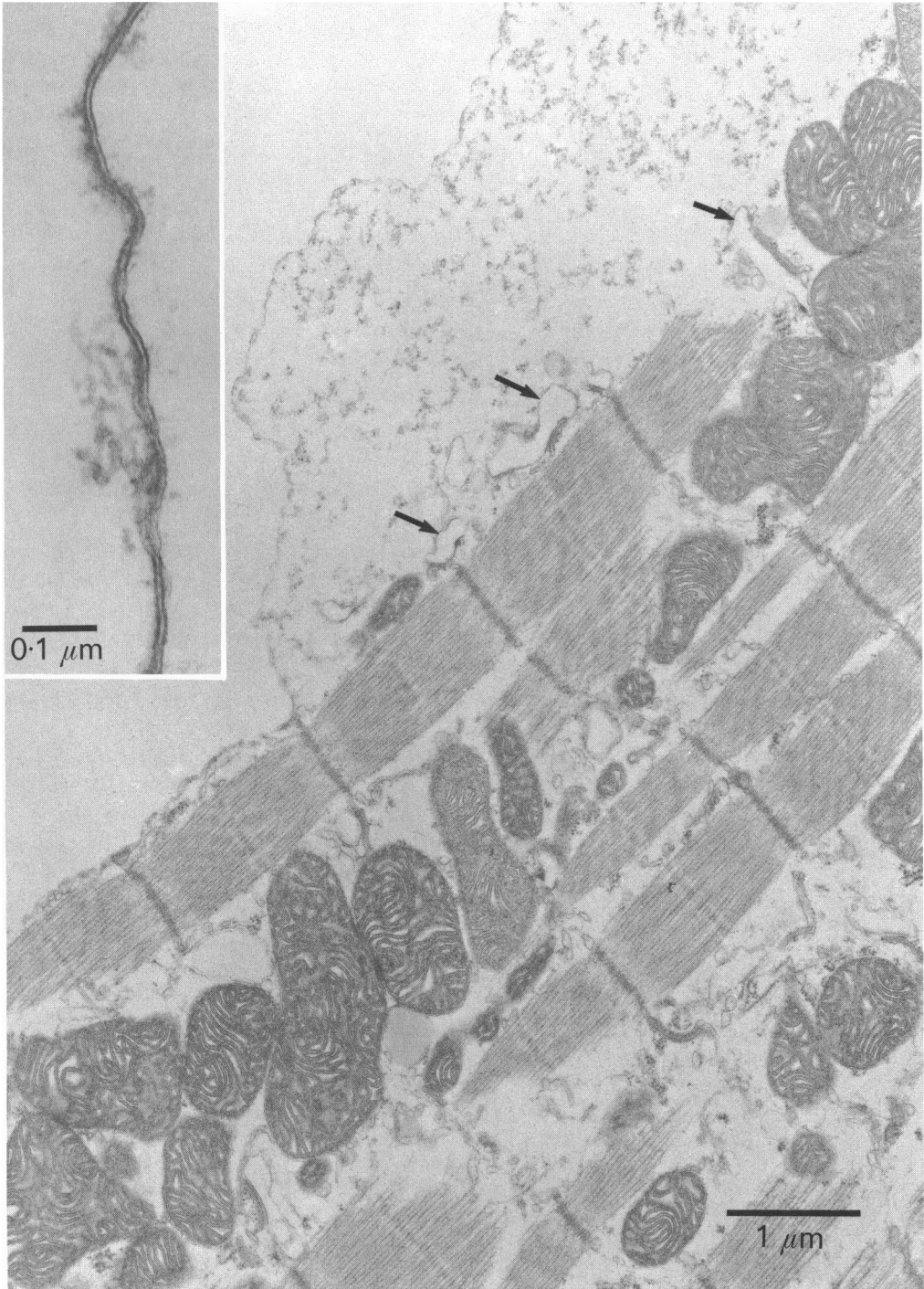


Fig. 18. For legend see page 52.